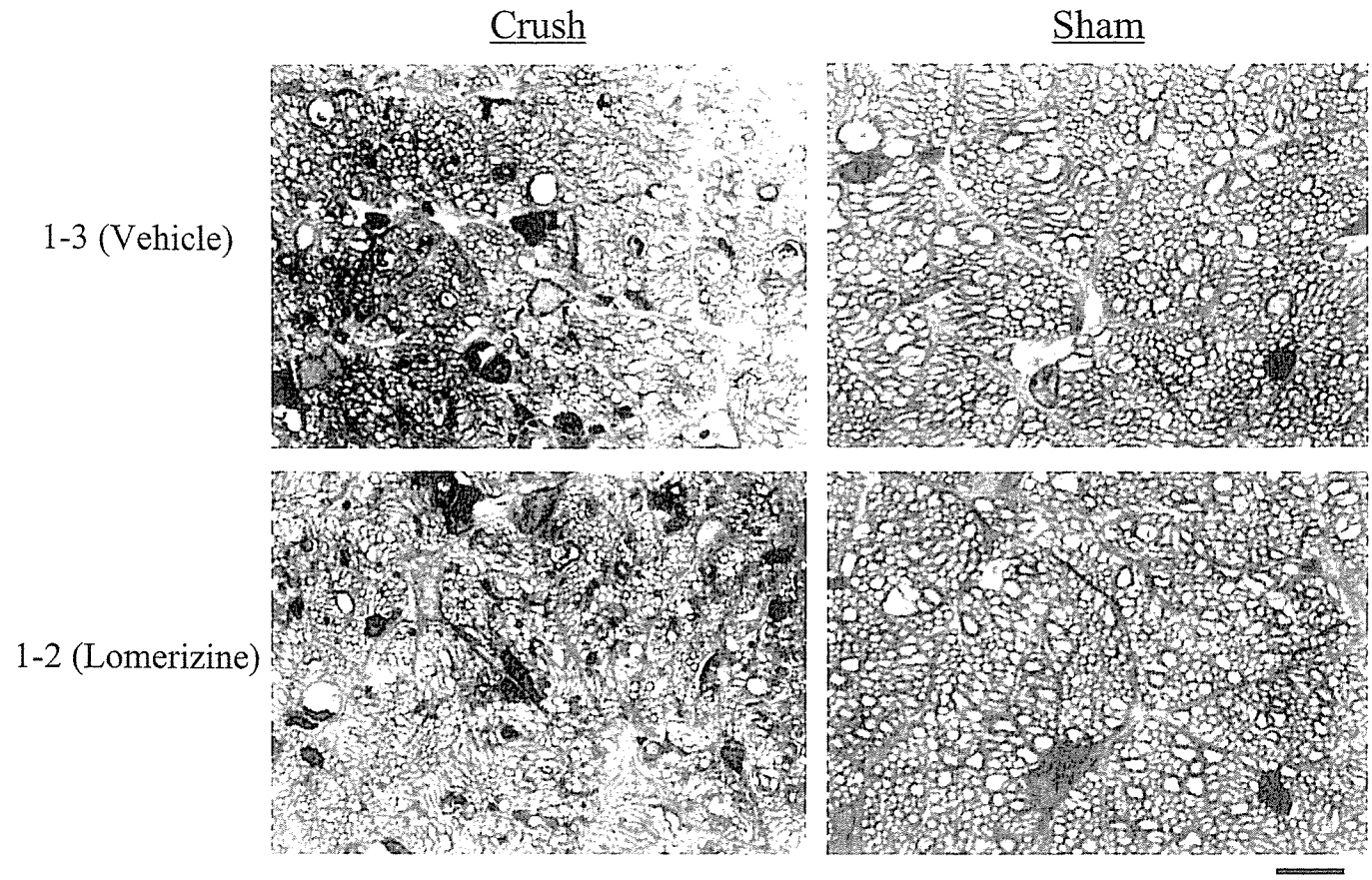

FIGURE 4 Representative light micrographs of RGC axons in the control and 30 mg/kg lomerizine-treated groups. The intact myelinated axons in the contralateral sham-operated optic nerves of each group showed a regular arrangement, whereas the optic nerve crushing induced a decrease in the number of myelinated axons and an increase in connective tissue in both groups. Although the crushed axons from rats that received 30 mg/kg of lomerizine showed a relatively preserved regularity of fiber arrangement, no fine arrangement was observed in the entire area.

changes in the rat retina in the vehicle-treated group, implying that our crush technique did not evoke extensive retinal ischemic disturbance, especially in the inner retinal layer. However, it has been reported that basic parameters such as the conductance velocity and amplitude of transmitted visual stimuli were impaired by lower crush forces and that more complex visual functions were conserved even with severe RGC loss.[29] In this study we found that, at the force exerted by a 60 gram clip, the electroretinogram remained unchanged, and the visual evoked potential showed a mild depression of amplitude over 4 weeks after the optic nerve crush (data not shown). Retinal function was not assessed by electrophysiological recordings in the current study, and further investigations will be required to elucidate both the morphological and functional aspects of the neuroprotective properties of lomerizine.

We found a statistically significant difference in the number of surviving RGCs among the three groups using whole-mounted retinae but not in retinal cross-sections, although the latter showed a tendency for enhanced RGC density with lomerizine treatment. In addition, in the vehicle-treated crushed eyes, there were many more RGCs identified in the cross sections (86.2%) than in the whole-mount specimens (65.9%). One explanation for this phenomenon is that it may reflect the smaller area of assessment created by the latter technique. The whole-mount technique makes it possible to assess the tracer-labeled RGCs in a wider area,[30] and the RGCs that we counted by this technique corresponded to approximately 15–20% of the total RGCs in the normal adult rat retina. The other possibility is that this phenomenon depends on variability between animals. However, the number of the FG-labeled RGCs in the uncrushed eyes of 21 rats ranged from 1238 to 1549 per mm^2, which would suggest that there is relatively little variability between animals. Further, this phenomenon might, at least in part, explain the impairment of retrograde axonal transport. Because the tracer fades over 3 weeks,[31] the FG was applied after the optic

nerve injury, a time at which we would expect diverse states in the neuronal cells. We found that not all the RGCs that survived the optic nerve injury maintained their capacity for retrograde axonal transport, and yet they survived.

The histological investigation of RGC axons revealed no significant alteration in the total number between the groups or their density, although the crushed axons that received 30 mg/kg lomerizine maintained the regularity of their fiber arrangement well compared with the vehicle-treated crushed eye group. The apparent discrepancy between the results on retrogradely labeled RGC numbers or those counted on retinal cross-sections and the density or total numbers of RGC axons could be explained by a spreading degeneration in the ganglion cell layer. After partial optic nerve injury, secondary degeneration of neurons that escaped primary injury does not necessarily begin at the axons near lesions; it may just as well begin in cell bodies adjacent to cell bodies of directly damaged axons that are in the process of dying.[28] Certainly, secondary degeneration could be due to the toxic effects of primarily dying RGC bodies in the retina, and several authors have described neuronal deaths distant from the lesion site.[32,33] However, Levkovitch-Verbin et al.[34] showed a greater proportional loss of optic nerve axons than RGC bodies at 3 months after ON transection in the monkey, and they concluded that this was evidence that the optic nerve was the site of secondary degeneration. Additionally, there is an interval of weeks between axonal injury and RGC death.[35] Taken together, our results suggest that the application of lomerizine ameliorated or maintained retrograde axonal transport in axons that escaped the initial injury but that secondary degeneration was still propagated.

Axonal injury induces various signs of pathological damage, including axon swelling,[36] proliferation of glial cells,[37] accumulation of endogenous T cells,[38] and perturbation of axonal transport.[39] Retrograde axonal transport is an essential process for delivering both extracellular components such as growth factors and intracellular components such as recycled synaptic vesicles from the nerve terminals to the cell bodies of neurons. Disturbance of the transport deprives the somata of various essential substances, eventually leading to the death of the neuron. It has been demonstrated that impairment of axonal transport can be induced by numerous pathological conditions including transient ischemia,[40] diabetes mellitus,[41] axotomy, optic nerve crush, acute IOP elevation,[42] and human glaucoma.[43] On the other hand, calcium regulates both the endocytosis and exocytosis of the synaptic vesicles and the retrograde axonal transport of proteins. *In vitro* studies have shown that a certain minimal level of Ca^{2+} is necessary to maintain both anterograde and retrograde transport.[44,45] However, impairment of Ca^{2+} homoeostasis is thought to play a vital role in triggering neuronal vulnerability models;[46] elevation of the Ca^{2+} concentration inhibits both anterograde[47] and retrograde transport of proteins.[48] Furthermore, it has been reported that betaxolol, a β-adrenoreceptor antagonist that is currently used worldwide in glaucoma therapy, showed a neuroprotective property in a rat ischemic model, presumably via inhibition of the voltage-gated calcium channels and the subsequent reduction in the intracellular calcium concentration.[49,50] Furthermore, another calcium channel antagonist, flunarizine, tended to alleviate retinal damage, but its effect did not reach statistical significance, according to Toriu et al.[26] Other investigators have reported that flunarizine diminished the retinal disturbance in identical or similar ischemic models.[51,52] However, it remains to be determined whether the maintenance of retrograde axoplasmic flow by the systemic application of lomerizine in the current study might reflect its direct or indirect action, secondary to the inhibition of the pathological cell response, including the activation of astrocytes and the subsequent formation of a glial scar.

In conclusion, we demonstrated that the long-term repeated administration of lomerizine rescued RGCs from secondary degeneration induced by optic nerve crush in the rat, presumably by maintaining or even improving the retrograde axonal transport. However, our findings did not elucidate the precise mechanism by which lomerizine exerts its neuroprotective effect. Further research will be required to elucidate the neuroprotective mechanism of lomerizine.

ACKNOWLEDGMENTS

This work was supported by a Grant-in-Aid for scientific research from the Ministry of Education, Culture, Sports, Science and Technology of Japan (15790980).

REFERENCES

[1] Adachi K, Kashii S, Masai H, et al. Mechanism of pathogenesis of glutamate neurotoxicity in retinal ischemia. *Graefes Arch Clin Exp Ophthalmol.* 1998;23:766–774.

[2] Buchi ER. Cell death in the rat retina after a pressure-induced ischemia reperfusion insult. An electron microscopic study: ganglion cell layer and inner nuclear layer. *Exp Eye Res.* 1992;55:605–613.
[3] Weber M, Bonaventure N, Sahel JA. Protective role of excitatory amino acid antagonists in experimental retinal ischemia. *Grafes Arch Exp Ophthalmol.* 1995;233:360–365.
[4] Wu SM, Maple BR. Amino acid neurotransmitters in the retina: a functional overview. *Vis Res.* 1998;38:1371–1384.
[5] Bloomfield SA, Dowling JE. Roles of aspartate and glutamate in synaptic transmission in rabbit retina. I. Outer plexiform layer. *J Neurophysiol.* 1985;53:699–713.
[6] Bloomfield SA, Dowling JE. Roles of aspartate and glutamate in synaptic transmission in rabbit retina. II. Inner plexiform layer. *J Neurophysiol.* 1985;53:714–725.
[7] Osborne NN, Ugarte M, Chao M, et al. Neuroprotection in relation to retinal ischemia and relevance to glaucoma. *Surv Ophthalmol.* 1999;43:S102–128.
[8] Melena J, Osborne NN. Voltage-dependent calcium channels in the rat retina: involvement in NMDA-stimulated influx of calcium. *Exp Eye Res.* 2001;72:393–401.
[9] Cohn JN. Calcium, vascular smooth muscle, and calcium entry blockers in hypertension. *Ann Intern Med.* 1983;98:806–809.
[10] Hof RP. Calcium antagonist and the peripheral circulation: differences and similarities between PY 108-068, nicardipine, verapamil, and diltiazem. *Br J Pharmacol.* 1982;78:375–394.
[11] Yamamoto T, Kitazawa Y. Vascular pathogenesis of normal-tension glaucoma: a possible pathogenetic factor, other than intraocular pressure, of glaucomatous optic neuropathy. *Prog Retin Eye Res.* 1998;17:127–143.
[12] Toriu N, Sasaoka M, Shimazawa M, et al. Effect of lomerizine, a novel Ca^{2+} channel blocker, on the normal and endothelin-1-disturbed circulation in the optic nerve head of rabbits. *J Ocul Pharmacol Ther.* 2001;17:131–149.
[13] Iwamoto T, Morita T, Kanazawa T, et al. Effect of KB-2796, a new calcium antagonist, and other diphenylpiperazines on [^{3}H]nitrendipine binding. *Jpn J Pharmacol.* 1988;48:241–247.
[14] Kanazawa T, Toda N. Inhibition by KB-2796, a new Ca^{2+} entry blocker, of the contractile response of isolated cerebral arteries in the dog. *Folia Pharmacol Jpn.* 1987;89:365–373.
[15] Kanazawa T, Nakasu Y, Matsuda M, Handa J. Acute effects of 1-[bis-(4-fluorophenyl)methyl]-4-(2,3,4-trimethoxybenzyl)-piperazine dihydrochloride, KB-2796, on cerebral blood flow in unanesthetized cats. *Arch Jpn Chir.* 1986;55:682–688.
[16] Yamada C, Harada K, Shimamoto A, et al. Effects of lomerizine on cerebral blood flow and systemic arterial blood pressure in anesthetized dogs. *Jpn Pharmacol Ther.* 1997;25:797–802.
[17] Akaike N, Ishibashi H, Hara H, et al. Effect of KB-2796, a new diphenylpiperazine Ca^{2+} antagonist, on voltage-dependent Ca^{2+} current and oxidative metabolism in dissociated mammalian CNS neurons. *Brain Res.* 1993;619:263–270.
[18] Hara H, Yokota K, Shimazawa M, Sukamoto T. Effect of KB-2796, a new diphenylpiperazine Ca^{2+} antagonist, on glutamate-induced neurotoxicity in rat hippocampal primary cell cultures. *Jpn J Pharmacol.* 1993;61:361–365.
[19] Hara H, Ozaki A, Yoshidomi M, Sukamoto T. Protective effect of KB-2796, a new calcium antagonist, in cerebral hypoxia and ischemia. *Arch Int Pharmacodyn Ther.* 1990;304:206–218.
[20] Levkovitch-Verbin H, Quigley HA, Martin KR, et al. A model to study differences between primary and secondary degeneration of retinal ganglion cells in rats by partial optic nerve transection. *Invest Ophthalmol Vis Sci.* 2003;44(8):3388–3393.
[21] Honjo M, Tanihara H, Kido N, et al. Expression of ciliary neurotrophic factor activated by retinal Muller cells in eyes with NMDA- and kainic acid-induced neuronal death. *Invest Ophthalmol Vis Sci.* 2000;41:552–560.
[22] Perry VH. Evidence for an amacrine cell system in the ganglion cell layer of the rat retina. *Neuroscience.* 1981;6:931–944.
[23] Dreyer EB, Zurakowski D, Schumer RA, et al. Elevated glutamate levels in the vitreous body of humans and monkeys with glaucoma. *Arch Ophthalmol.* 1996;114:299–305.
[24] Sucher NJ, Lei SZ, Lipton SA. Calcium channel antagonists attenuate NMDA receptor-mediated neurotoxicity of retinal ganglion cells in culture. *Brain Res.* 1991;551:297–302.
[25] Weiss JH, Hartley DM, Koh J, Choi DW. The calcium channel blocker nifedipine attenuates slow excitatory amino acid neurotoxicity. *Science* 1990;247:1474–1477.
[26] Toriu N, Akaike A, Yasuyoshi H, et al. Lomerizine, a Ca^{2+} channel blocker, reduces glutamate-induced neurotoxicity and ischemia/reperfusion damage in rat retina. *Exp Eye Res.* 2000;70:475–484.
[27] Schwartz M. Optic nerve crush: protection and regeneration. *Brain Res Bull.* 2004;62:467–471.
[28] Yoles E, Muller S, Schwartz M. NMDA-receptor antagonist protects neurons from secondary degeneration after partial optic nerve crush. *J Neurotrauma.* 1997;14:665–675.
[29] Klocker N, Zerfowski M, Gellrich NC, Bahr M. Morphological and functional analysis of an incomplete CNS fiber tract lesion: graded crush of the rat optic nerve. *J Neurosci Methods.* 2001;110:147–153.
[30] Sawada A, Neufeld AH. Confirmation of the rat model of chronic, moderately elevated intraocular pressure. *Exp Eye Res.* 1999;69:525–531.
[31] Selles-Navarro I, Villegas-Perez MP, Salvador-Silva M, et al. Retinal ganglion cell death after different transient periods of pressure-induced ischemia and survival intervals: a quantitative in vivo study. *Invest Ophthalmol Vis Sci.* 1996;37:2002–2014.
[32] Barres BA, Jacobson MD, Schmid R, et al. Does oligodendrocyte survival depend on axons? *Curr Biol.* 1993;3(8):489–497.
[33] Crowe MJ, Bresnahan JC, Shuman SL, et al. Apoptosis and delayed degeneration after spinal cord injury in rats and monkeys. *Nat Med.* 1997;3(1):73–76.
[34] Levkovitch-Verbin H, Quigley HA, Kerrigan-Baumrind LA, et al. Optic nerve transection in monkeys may result in secondary degeneration of retinal ganglion cells. *Invest Ophthalmol Vis Sci.* 2001;42(5):975–982.
[35] Berkelaar M, Clarke DB, Wang YC, et al. Axotomy results in delayed death and apoptosis of retinal ganglion cells in adult rats. *J Neurosci.* 1994;14(7):4368–4374.
[36] Maxwell WL, Watt C, Graham DI, Gennarelli TA. Ultrastructural evidence of axonal shearing as a result of lateral acceleration of the head in non-human primates. *Acta Neuropathol.* 1993;86:136–144.
[37] Maeda K, Sawada A, Matsubara M, et al. A novel neuroprotectant against retinal ganglion cell damage in a glaucoma model and an optic nerve crush model in the rat. *Invest Ophthalmol Vis Sci.* 2004;45:851–856.
[38] Moalem G, Monsonego A, Shani Y, et al. Differential T cell response in central and peripheral nerve injury: connection with immune privilege. *FASEB J.* 1999;13:1207–1217.
[39] McKerracher L, Hirscheimer A. Slow transport of the cytoskeleton after axonal injury. *J Neurobiol.* 1992;23:568–578.
[40] Lafuente Lopez-Herrera MP, Mayor-Torroglosa S, Miralles de Imperial J, et al. Transient ischemia of the retina results in altered retrograde axoplasmic transport: neuroprotection with brimonidine. *Exp Neurol.* 2002;178:243–258.
[41] Zhang L, Inoue M, Dong K, Yamamoto M. Retrograde axonal transport impairment of large-and medium-sized retinal ganglion cells in diabetic rat. *Curr Eye Res.* 2000;20:131–136.
[42] Minckler DS, Bunt AH, Johanson GW. Orthograde and retrograde axoplasmic transport during acute ocular hypertension in the monkey. *Invest Ophthalmol Vis Sci.* 1977;16:426–441.

[43] Quigley HA, Addicks EM, Green WR, Maumenee AE. Optic nerve damage in human glaucoma. II. The site of injury and susceptibility to damage. *Arch Ophthalmol.* 1981;99:635–649.
[44] Chan SY, Ochs S, Worth RM. The requirement for calcium ions and the effect of other ions on axoplasmic transport in mammalian nerve. *J Physiol.* 1980;301:477–504.
[45] Johansson JO. Influence of low IOP and low calcium on retrograde axoplasmic transport in rat optic nerve in vitro. *Exp Eye Res.* 1985;41:739–744.
[46] Taft WC, Clifton GL, Blair RE, DeLorenzo RJ. Phenytoin protects against ischemia-produced neuronal cell death. *Brain Res.* 1989;483:143–148.
[47] Brady ST, Crothers SD, Nosal C, McClure WO. Fast axonal transport in the presence of high $Ca2^{+}$: evidence that microtubules are not required. *Proc Natl Acad Sci USA.* 1980;77:5909–5913.
[48] Lees GJ. Inhibition of the retrograde axonal transport of dopamine-beta-hydroxylase antibodies by the calcium ionophore A23187. *Brain Res.* 1985;345:62–67.
[49] Osborne NN, Cazevielle C, Carvalho AL, et al. In vivo and in vitro experiments show that betaxolol is a retinal neuroprotective agent. *Brain Res.* 1997;751:113–123.
[50] Osborne NN, DeSantis L, Bae JB, et al. Topically applied betaxolol attenuates NMDA-induced toxicity to ganglion cells and the effects of ischaemia to the retina. *Exp Eye Res.* 1999;69:331–342.
[51] Takahashi K, Lam TT, Edward DP, et al. Protective effects of flunarizine on ischemic injury in the rat retina. *Arch Ophthalmol.* 1992;110:862–870.
[52] Eschweiler GW, Bahr M. Flunarizine enhances rat retinal ganglion cell survival after axotomy. *J Neurosci Sci.* 1993;116:34–40.

Metallothionein, an Endogenous Antioxidant, Protects against Retinal Neuron Damage in Mice

Shinsuke Suemori,[1,2] *Masamitsu Shimazawa,*[1] *Kazuhide Kawase,*[2] *Masahiko Satoh,*[3] *Hisamitsu Nagase,*[3] *Tetsuya Yamamoto,*[2] *and Hideaki Hara*[1]

Purpose. To clarify the functional role of metallothionein (MT) in retinal damage in mice deficient in both MT-I and -II (MT-I/-II-deficient mice [C57BL/6J background]) and wild-type (C57BL/6J) mice and MT induction (zinc sulfate [$ZnSO_4$] and 1α, 25-dihydroxyvitamin D_3 [Vit. D_3]).

Methods. Retinal, cell damage was induced by intravitreous injection of *N*-methyl-D-aspartate (NMDA; 40 nmol/eye). Retinal MT-I, -II, and -III mRNA expression was monitored by real-time reverse-transcription-PCR of total retinal RNA from eyes injected or not injected with NMDA. In wild-type mice, MT-I and -II immunohistochemistry was performed (with antibody that recognizes both proteins) 12 and 24 hours after intravitreous NMDA injection. To examine the involvement of induced retinal MT, $ZnSO_4$ (10 nmol/eye) or Vit. D_3 (0.2 or 2 ng/eye) was intravitreously injected 24 hours before NMDA injection in wild-type or MT-I/-II-deficient mice, and ganglion cell layer (GCL) cell loss and inner plexiform layer (IPL) thinning were evaluated 7 days after the NMDA injection. The protective effect of Vit. D_3 was assessed against the RGC-5 cell death induced by oxidative stress (using buthionine sulfoximine [BSO] to deplete glutathione in combination with glutamate to inhibit cystine uptake).

Results. In wild-type mice, MT-II mRNA expression was time-dependently elevated by NMDA (5.9 and 7.4 times versus the nontreated control at 4 and 12 hours, respectively, after injection), with the normal level being regained within 24 hours. In contrast, MT-I and -III showed persistent decreases (to <50% control) from 4 to 24 hours. In wild-type mice, MT-like immunoreactivity was increased in the inner retina (GCL and IPL) 12 and 24 hours after NMDA injection. At 7 days after NMDA injection in MT-I/-II-deficient mice (versus wild-type mice), GCL cell loss was increased, but IPL thickness was not different. Pretreatment with $ZnSO_4$ or Vit. D_3 increased inner retinal MT-like immunoreactivity 24 hours after NMDA injection and significantly attenuated NMDA-induced GCL cell loss in wild-type mice, but $ZnSO_4$ pretreatment did not protect against such cell loss in MT-I/-II-deficient mice. In vitro, Vit. D_3 pretreatment (100 nM) reduced BSO+glutamate-induced RGC-5 cell death.

Conclusions. These findings suggest that MT, especially MT-II, protects against retinal neuron damage, by acting as an endogenous antioxidant. (*Invest Ophthalmol Vis Sci.* 2006;47:3975-3982) DOI:10.1167/iovs.06-0275

Retinal ganglion cell death is a common feature of ophthalmic disorders such as glaucoma and central artery and vein occlusion. In humans and monkeys, glaucoma is associated with a significant elevation in the vitreous glutamate concentration.[1] Retinal ganglion cells are exquisitely sensitive to the effects of both glutamate and its analogue *N*-methyl-D-aspartate (NMDA), which produces a dose-dependent cell loss both in vivo and in vitro, and glutamate toxicity has been implicated in the pathophysiology of glaucoma.[2] NMDA receptor-mediated neurotoxicity has been reported to depend in part on the generation of nitric oxide and superoxide anions, which react to form peroxynitrite.[3] Thus, oxidative stress, leading to the formation of free radicals, has been implicated as part of the final common pathway for neurotoxicity in a wide variety of acute and chronic neurodegenerative diseases.[4-6]

In contrast, all aerobic cells possess an antioxidant defense system that has enzymatic and nonenzymatic components. The enzymatic component comprises three major enzymes: superoxide dismutase, glutathione peroxidase, and catalase. The nonenzymatic component includes vitamins A and E and also glutathione (GSH), a key component of the cell-defense system.[7,8] Abnormally low levels of GSH have been reported in the lens[9] and whole blood of patients with age-related cataract[10] and in the blood of patients with glaucoma,[11] proliferative diabetic retinopathy (PDR), proliferative vitreoretinopathy (PVR),[12] or age-related macular degeneration (ARMD).[13] Thus, in several retinal diseases, decreases in GSH could reduce the scavenging capacity against reactive oxygen species, causing an increased vulnerability of neurons.

Metallothionein (MT) is a class consisting of four low-molecular-weight (6000-7000), metal-binding proteins with a high cysteine content.[14] These MT isoforms are known as MT-I, -II, -III, and -IV,[15-17] and they serve as important regulators of metal homeostasis and as a source of the zinc incorporated into proteins, including transcription factors.[18] Several studies have found that MT has a free-radical-scavenging function in tissues subjected to oxidative stress and that it affords cytoprotection via this radical-scavenging ability.[19-22] Of interest, it has been reported that the expressions of MT-I and -II, but not that of MT-III, increase after cerebral ischemia and that MT-I isoform-overexpressing transgenic mice have a reduced infarct size after cerebral ischemia.[23,24] These findings suggest that MT may be an important neuroprotective substance for stroke and other acute neurodegenerative diseases. However, little is known about the functional role of MT in retinal diseases.

In the present study, we monitored the time course of changes in the expressions of MT isoforms (MT-I, -II, and -III mRNAs) and in the distribution of MT proteins during retinal damage in mice. In addition, we used mice deficient in both MT-I and -II and two inducers of MT (zinc and 1α, 25-dihydroxyvitamin D_3) to clarify the role played by MT in retinal neurons.

From the Departments of [1]Biofunctional Molecules and [3]Hygieiology, Gifu Pharmaceutical University, Gifu, Japan; and the [2]Department of Ophthalmology, Gifu University Graduate School of Medicine, Gifu, Japan.

Supported by a research grant from the Imai Memorial Glaucoma Foundation.

Submitted for publication March 14, 2006; revised April 30, 2006; accepted June 26, 2006.

Disclosure: **S. Suemori**, None; **M. Shimazawa**, None; **K. Kawase**, None; **M. Satoh**, None; **H. Nagase**, None; **T. Yamamoto**, None; **H. Hara**, None

The publication costs of this article were defrayed in part by page charge payment. This article must therefore be marked "*advertisement*" in accordance with 18 U.S.C. §1734 solely to indicate this fact.

Corresponding author: Hideaki Hara, Department of Biofunctional Molecules, Gifu Pharmaceutical University, 5-6-1 Mitahora-higashi, Gifu 502-8585, Japan; hidehara@gifu-pu.ac.jp.

Materials and Methods

Animals

Male metallothionein-I and -II (MT-I/-II)-deficient[25] and wild-type mice weighing 20 to 25 g were used in the present study. The background strain of mice was C57BL/6J, and this strain was used as the wild-type control. All experiments were performed in accordance with the ARVO Statement for the Use of Animals in Ophthalmic and Vision Research and were approved and monitored by the Institutional Animal Care and Use Committee of Gifu Pharmaceutical University.

Intravitreal Injection

Mice were anesthetized with 3.0% isoflurane, then maintained using 1.5% isoflurane in 70% N_2O and 30% O_2 using an animal general anesthesia machine (Soft Lander, Sin-ei Industry Co. Ltd., Saitama, Japan). Intravitreal injections (2 μL) were performed using a 32-gauge needle 0.5 mm behind the limbus in the inferior region of the globe, through the conjunctiva and sclera. Eyes were routinely injected with 2 μL of 20 mM NMDA (40 nmol/eye; Sigma-Aldrich, St. Louis, MO). Any mice that exhibited postoperative complications, such as retinal hemorrhage, vitreous hemorrhage, or retinal detachment, were excluded from the analysis.

In another series of experiments, zinc sulfate ($ZnSO_4$, 10 nmol/eye; Wako, Osaka, Japan) or 1α, 25-dihydroxyvitamin D_3 (Vit. D_3, 2 ng/eye; Biomol, Plymouth Meeting, PA), each of which induces MT expression (or vehicle; and identical dose of sulfuric acid or ethanol in saline served as the respective control) was intravitreously injected 24 hours before the NMDA injection in wild-type or MT-I/-II deficient mice. The time point for administration of MT inducers chosen to be 24 hours before the NMDA injection, because the intravitreous injection of Vit. D_3 (2 ng/eye) sufficiently increased MT-like immunoreactivity in retina at 24 hours, as mentioned later.

Histology

The mice were euthanatized by inhalation of diethyl ether at the end of the experiment. Each eye was enucleated and postfixed overnight in 4% paraformaldehyde solution in 0.1 M phosphate buffer (pH 7.4) at 4°C and embedded in paraffin. Six paraffin-embedded sections (thickness, 4 μm) cut through the optic disc of each eye were prepared in a standard manner and stained with hematoxylin and eosin. Retinal damage was evaluated as described previously,[26] with three sections from each eye being used for the morphometric analysis. Light microscope images were photographed, and the cell counts in the ganglion cell layer (GCL) at a distance between 350 and 650 μm from the optic disc, and the thickness of the inner plexiform layer (IPL) were measured on the micrographs in a masked fashion by a single observer (SS). Data from three sections (selected randomly from the six sections) were averaged for each eye and used to evaluate the GCL cell count and the IPL thickness.

Real-time RT-PCR

Retinas were obtained from wild-type mice before and at 4, 12, and 24 hours after the NMDA injection. Total RNA was isolated from these retinas using an SV total RNA isolation system (Promega, Madison, WI). Quantitative real-time PCR, after reverse transcription, was performed to determine the time-course of changes in the gene expression of MT isoforms (MT-I, -II, and -III). Briefly, 1 μg total RNA was used for first-strand cDNA synthesis (SuperScript II reverse transcriptase; Invitrogen, Carlsbad, CA) with Oligo (dT) 12 to 18 primer (Invitrogen), in accordance with the manufacturer's instructions. Real-time PCR was performed in 50 μL of reaction mixture containing each primer (see Table 1), template cDNA, and supermix (SYBR Green; Bio-Rad, Hercules, CA) using a single-color real-time PCR detection system (MyiQ; Bio-Rad) according to the manufacturer's instructions. Reactions were performed in 40 cycles consisting of 15 seconds' denaturation (94°C) and 60 seconds' elongation with annealing (60°C). β-Actin was used as the reference standard, and relative levels of MT isoforms compared with that of β-actin were calculated.

Table 1. Primer Sequences for Metallothionein Isoforms and β-Actin

Name	Primer (5′–3′)	Product Size (bp)
MT-I	Forward: ggtcctctaagcgtcaccac	102
	Reverse: gagcagttggggtccattc	
MT-II	Forward: cctgtgcctccgatggat	153
	Reverse: acttgtcggaagcctctttg	
MT-III	Forward: ctgagacctgcccctgtc	181
	Reverse: ttctcggcctctgccttg	
β-Actin	Forward: gatctggcaccacaccttct	138
	Reverse: ggggtgttgaaggtctcaaa	

Immunohistochemistry

To detect MT protein expression in the retina, MT immunostaining was performed. A total of 24 animals was used and divided into four groups: nontreated in wild-type mice (n = 6), nontreated in MT-I/II-deficient mice (n = 6), 12 hours after NMDA (40 nmol/eye) injection in wild-type mice (n = 6), and 24 hours after NMDA (40 nmol/eye) injection in wild-type mice (n = 6). Eyes were then postfixed overnight in 4% paraformaldehyde solution in 0.1 M phosphate buffer (pH 7.4) at 4°C, and embedded in paraffin. Horizontal sections (4 μm) through the optic nerve were obtained from the paraffin-embedded eyes. Such sections were deparaffinized with xylene and dehydrated through a graded ethanol series. Immunohistochemical staining was performed in accordance with the protocol provided for a commercially available immunohistologic staining kit (Histomouse-Plus Kits; Zymed Laboratories Inc., South San Francisco, CA). Briefly, tissue sections were washed in a 0.01 M phosphate-buffered saline solution (PBS) for 10 minutes, and then endogenous peroxidase was quenched by treating the sections with 3% hydrogen peroxide in absolute methanol for 10 minutes. After the sections were washed with PBS, they were incubated with blocking solutions A and B for 30 and 10 minutes, respectively, to eliminate nonspecific background. After the sections were washed with PBS, a mouse monoclonal antibody against MT-I and -II proteins (clone E9; Zymed Laboratories Inc.) was added at a dilution of 1.100, and incubation was allowed to proceed for 60 minutes. After the sections were washed with PBS, a biotinylated secondary antibody was added, and the sections were incubated for 30 minutes. After the sections were washed with PBS, streptavidin-peroxidase was added, incubated for 20 minutes, and visualized as a red deposit by addition of a chromogen solution substrate. Omission of primary antibodies served as a negative control. The level of MT-like immunoreactivity in retina was estimated compared with that in corneal endothelium in each specimen.

For induction of MT protein in the retina, $ZnSO_4$ (10 nmol/eye), Vit. D_3 (0.2 ng and 2 ng/eye; or vehicle [see above] as control) was intravitreously injected in wild-type mice. Twenty-four hours later, the upregulation of MT protein was detected using the immunostaining described earlier. The concentrations achieved in the vitreous body after intravitreous injections of $ZnSO_4$ and low- and high-dose Vit. D_3 were estimated to be 1 mM, 20 ng/mL, and 200 ng/mL, respectively. The doses of these inducers used in this study were chosen by reference to previous studies in which $ZnSO_4$ and Vit. D_3 were reported to induce MT-I and -II mRNA expressions.[27,28]

RGC-5 Culture

Cultures of RGC-5 cells were maintained in Dulbecco's modified Eagles's medium (D-MEM; Sigma-Aldrich) supplemented with 10% fetal bovine serum (FBS; Valeant, Costa Mesa, CA), 100 U/mL penicillin (Meiji Seika Kaisha, Ltd., Tokyo, Japan), and 100 μg/mL streptomycin (Meiji Seika Kaisha, Ltd.) in a humidified atmosphere of 95% air and 5%

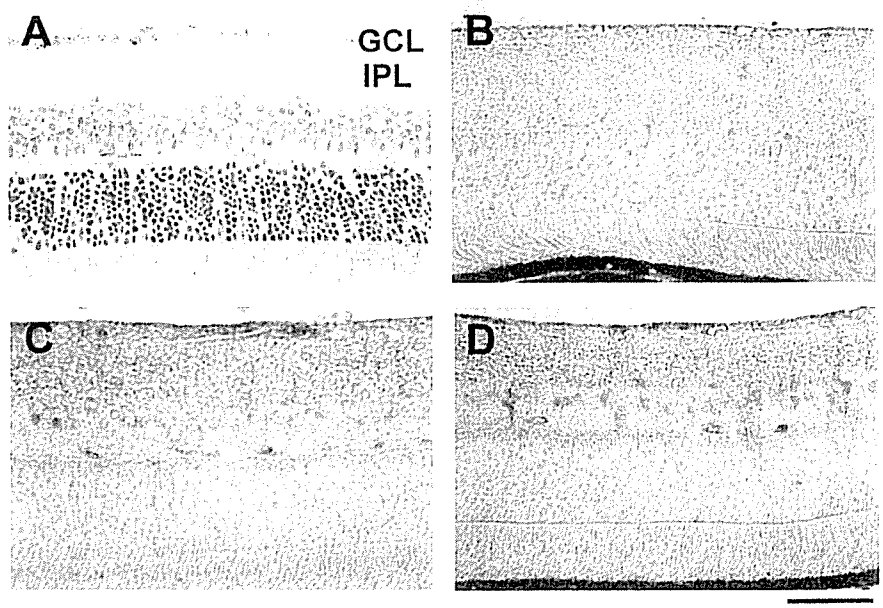

FIGURE 1. Distribution of MT-like immunoreactivity in mouse retina after NMDA injection. Retinal cross sections were labeled with antibody against MT. (**A**) Hematoxylin and eosin staining, (**B**) control (nontreated normal retina), (**C**) 12 hours after intravitreous injection of NMDA in wild-type mice, (**D**) 24 hours after intravitreous injection of NMDA in wild-type mice. MT-like immunoreactivity was increased in the inner retina at both 12 and 24 hours after intravitreous injection of NMDA at 40 nmol/eye. Scale bar, 50 μm.

CO_2 at 37°C. The RGC-5 cells were passaged by trypsinization every 3 days, as in our previous report.[26]

Cell Mortality Assay after Oxidative Stress

For induction of oxidative stress in an RGC-5 cell culture in vitro, buthionine sulfoximine (BSO) and a high dose of glutamate (10 mM) were added to the cell culture medium, as previously described by Maher and Hanneken.[29] BSO, a glutamate-cysteine ligase inhibitor, inhibits GSH synthesis, resulting in a depletion of intracellular GSH, whereas high-dose glutamate inhibits the uptake of cystine, a rate-limiting amino acid in GSH synthesis. Such coadministration of BSO and glutamate induces cell death through an oxidative-stress pathway.

RGC-5 cells were plated at a density of 1000 cells/well in 96-well culture plates (3072; Falcon; BD Biosciences, Bedford, MA). Cells were washed twice with D-MEM, then with the same medium supplemented with 1% FBS+Vit. D_3 at 10 or 100 nM or with vehicle (0.1% ethanol). One hour later, BSO (500 μM; Wako) plus 10 mM glutamate (Nakarai Tesque, Inc., Kyoto, Japan) or vehicle (D-MEM), was added to each medium. Forty-eight hours after this addition, cell viability was measured using nuclear staining methods. Briefly, cell death was assessed on the basis of combination-staining with fluorescent dyes (Hoechst 33342; Invitrogen, Eugene, OR; and YO-PRO-1; Invitrogen), by inverted epifluorescence microscope (IX70; Olympus, Tokyo, Japan). At the end of the culture period, Hoechst 33342 and YO-PRO-1 dyes were added to the culture medium at 8 and 0.1 μM, respectively, for 30 minutes. Images were collected with a cooled charge-coupled device [CCD] camera (Olympus). In a blind manner, at least 400 cells per condition were counted with image-processing software (Image-J ver. 1.33f; National Institutes of Health). Cell mortality was quantified by determining the percentage of YO-PRO-1-positive cells to Hoechst 33342-positive cells.

Statistical Analysis

Data are presented as the mean ± SEM. Statistical comparisons were made by using a Student's *t*-test or Dunnett test (Stat View ver. 5.0; SAS Institute Inc., Cary, NC). $P < 0.05$ was considered to indicate statistical significance.

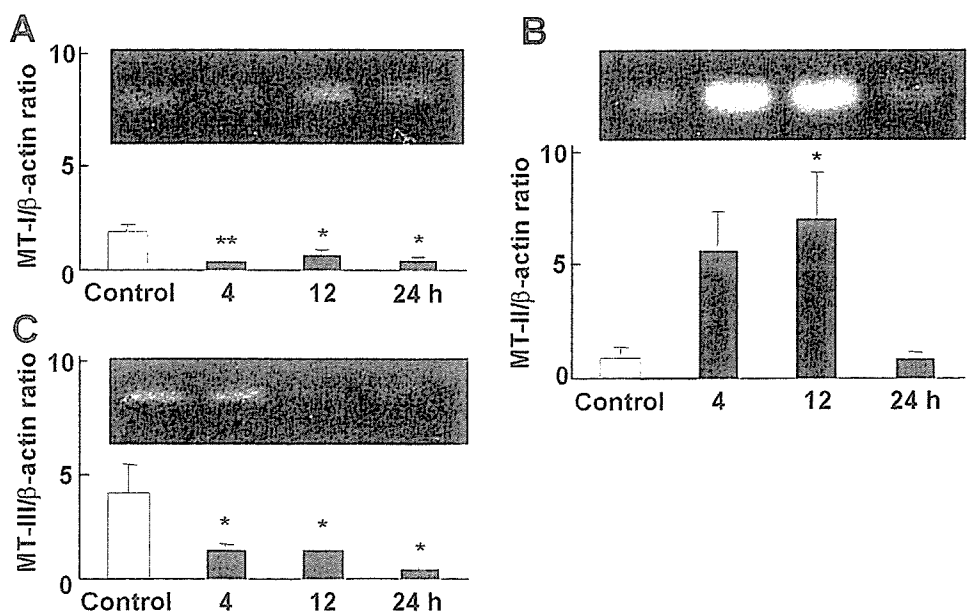

FIGURE 2. Time-course data for changes in MT-I, -II, and -III mRNAs in mouse retina after NMDA injection. Expressions of MT mRNAs in the retina were measured using a quantitative real-time reverse-transcriptase PCR assay at 4, 12, and 24 hours after intravitreous injection of NMDA (40 nmol) in wild-type mice. Data are the mean ± SEM of results in four animals. (**A**) MT-I, (**B**) MT-II, (**C**) MT-III. $^{*}P < 0.05$, $^{**}P < 0.01$ versus control (nontreated control retina Dunnett test).

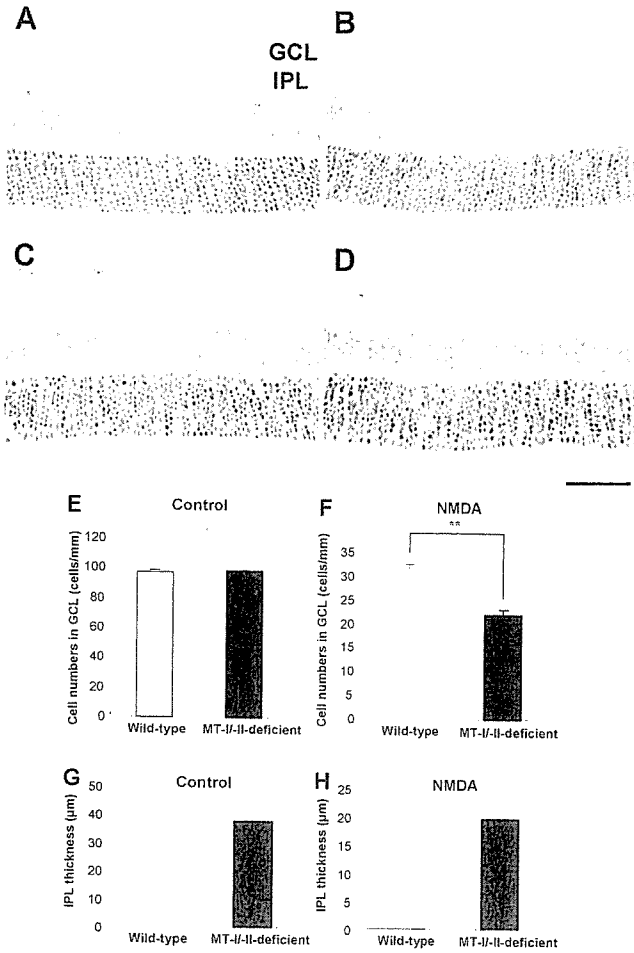

FIGURE 3. Retinal damage in MT-deficient or wild-type mice after NMDA injection. Retinal cross sections were prepared 7 days after intravitreous injection of NMDA (40 nmol) or vehicle. (**A**) Vehicle-treated control retina from wild-type mice, (**B**) NMDA-treated retina from wild-type mice, (**C**) vehicle-treated retina from MT-deficient mice, (**D**) NMDA-treated retina from MT-deficient mice. Scale bar, 50 μm. Retinal damage was evaluated by counting the number of cells in the GCL (**E**, **F**) and measuring the thickness of the IPL (**G**, **H**) in mice at 7 days after intravitreous injection of either NMDA (40 nmol, **F**, **H**) or vehicle (**E**, **G**). (□) Wild-type mice and (■) MT-deficient mice. Data are the mean ± SEM of results in nine animals. $^{**}P < 0.01$ versus wild-type mice (Student's *t*-test). GCL, ganglion cell layer; IPL, inner plexiform layer.

RESULTS

Expression of Metallothioneins

To clarify the changes in MT protein in the retina after retinal injury, MT expression was examined before and after an intravitreous injection of NMDA. For this, we used immunostaining with a specific antibody recognizing both MT-1 and -II proteins. Normal retina stained with hematoxylin and eosin is shown in Figure 1A for reference.

In the normal retina of wild-type mice before NMDA injection, MT-like immunoreactivity was localized to the retinal nerve fiber layer (RNFL) and inner plexiform layer (IPL), but was only slight (Fig. 1B) compared with that in the cornea. No MT-like immunoreactivity was observed in the retina of MT-I/-II-deficient mice (data not shown). Intravitreal injection of NMDA at 40 nmol/eye increased the MT-like immunoreactivity in the inner retina at 12 and 24 hours after the injection (Figs. 1C, 1D). Marked increases in MT-like immunoreactivity were observed in RNFL and in cells in the ganglion cell layer (GCL).

The time course of changes in the mRNA expressions for MT isoforms (MT-I, -II, and -III) after NMDA injection was examined in the retina of wild-type mice by real-time RT-PCR (Fig. 2). The MT-II mRNA level was time-dependently elevated 5.9- and 7.4-fold ($P < 0.05$) versus the nontreated control at 4 and 12 hours, respectively, after the NMDA injection (Fig. 2B), and it returned to the normal level by 24 hours. In contrast, MT-I and -III mRNA showed persistent decreases (to less than half the relevant control) from 4 to 24 hours (Figs. 2A, 2C).

Exacerbated NMDA-Induced Retinal Damage in MT-I/-II–Deficient Mice

The participation of MT in retinal cell damage was examined by comparing MT-I/-II-deficient mice with the wild-type mice. As shown in Figure 3, MT-I/-II-deficient mice showed a smaller number of cells in the GCL (22.1 ± 1.1 cells/mm, $n = 9$) at 7 days after the NMDA injection than in wild-type mice (31.6 ± 1.0 cells/mm, $n = 9$) ($P < 0.01$). However, no significant difference in IPL thickness was observed between MT-I/-II-deficient (19.8 ± 0.3 μm, $n = 9$) and wild-type mice (19.8 ± 0.4 μm, $n = 9$). In contrast, there were no significant differences in the number of GCL cells or IPL thickness between MT-I/-II-deficient (97.9 ± 1.7 cells/mm for GCL and 37.7 ± 0.5 μm for IPL, $n = 9$) and wild-type mice in retinas obtained from nontreated control eyes (97.3 ± 1.5 cells/mm for GCL and 36.7 ± 0.7 μm for IPL, $n = 9$).

Protective Effect of Increases in MT-I/II Induced by Zinc Ion or Vit. D_3 against NMDA-Induced Retinal Damage

To clarify the protective effects of MT against retinal injury, MT was induced either by zinc sulfate ($ZnSO_4$) or by Vit. D_3. Twenty-four hours after intravitreous injection of $ZnSO_4$ at 10 nmol/eye or of Vit. D_3 at 0.2 or 2 ng/eye in wild-type mice, MT-like immunoreactivity was markedly elevated in the inner retina (versus the vehicle-treated retina; Figs. 4B, 4C, 5). In contrast, no immunoreactivity was observed in retinas treated without the primary antibody (Fig. 4A).

The effects of $ZnSO_4$ on retinal damage in MT-I/-II-deficient mice and wild-type mice are summarized in Figure 6. In wild-type mice, treatment with $ZnSO_4$ at 24 hours before the NMDA injection significantly protected against cell loss in the GCL (versus the vehicle-treated NMDA control group; Figs. 6A–C, 6G), although no significant difference in IPL thickness was observed between $ZnSO_4$-treated (22.2 ± 1.0 μm, $n = 5$) and vehicle-treated groups (21.6 ± 0.9 μm, $n = 8$). In contrast, no protective effect of $ZnSO_4$ was evident in MT-I/-II-deficient mice (Figs. 6D–6G). The effects of Vit. D_3 on retinal damage in wild-type mice are shown in Figure 7. Treatment with Vit. D_3 at 24 hours before the NMDA injection significantly protected against cell loss in GCL (versus the vehicle-treated NMDA control group; Figs. 7A–D), although no significant difference in IPL thickness was observed between the Vit. D_3-pretreated (20.0 ± 0.3 μm, $n = 10$) and vehicle-treated groups (19.4 ± 0.4 μm, $n = 11$; Figs. 7B, 7C, 7E).

Effect of Vit. D_3 on Retinal Cell Death Induced by Oxidative Stress

Representative fluorescence nuclear staining using Hoechst 33342 and YO-PRO-1 dyes are shown in Figure 8A. In vehicle-treated control cells, we observed normal nuclear morphology and negative staining with YO-PRO-1 dye (which stains early apoptotic and later-stage cells). Cells treated for 48 hours with a combination of BSO (which inhibits glutamate cysteine ligase) and glutamate (which inhibits the uptake of cystine) revealed shrinkage and condensation of their nuclei and posi-

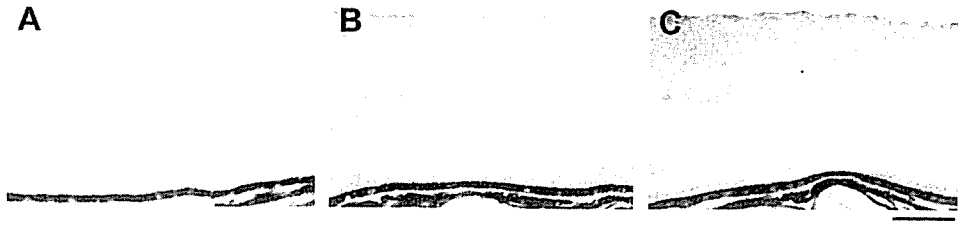

FIGURE 4. Effect of $ZnSO_4$ on MT-like immunoreactivity of mouse retina. Retinal cross sections were labeled with a primary antibody against MT in wild-type mice. Twenty-four hours after intravitreous injection of vehicle (A) without or (B) with the primary antibody; (C) 24 hours after intravitreous injection of $ZnSO_4$ (10 nmol). Scale bar, 50 μm.

tive staining with both YO-PRO-1 and Hoechst 33342 dyes. The number of cells exhibiting YO-PRO-1 fluorescence was counted, and positive cells were expressed as the percentage of YO-PRO-1-positive to Hoechst 33342-positive cells (Fig. 8B). The combination of 500 μM BSO and 10 mM glutamate induced significant cell death, the resulting percentage of YO-PRO-1-positive cells being 57.1% ± 3.2% (n = 8), whereas in the vehicle-treated control group, it was 0.9% ± 0.2% (n = 8). Pretreatment with Vit. D_3 at 100 nM, but not at 10 nM, significantly inhibited the cell death (approximately 20% inhibition) induced by the combination of BSO and glutamate. In contrast, treatment with Vit. D_3 alone at 100 nM had no effect on cell viability (versus the vehicle-treated control group; Fig 8B).

DISCUSSION

The present study, performed to assess the functional roles played by MT in retinal damage, used MT-I/-II-deficient mice and two inducers of MT. Intravitreal injection of NMDA increased the MT-like immunoreactivity in the inner retina of wild-type mice at both 12 and 24 hours (Figs. 1C, 1D). In particular, marked increases in MT-like immunoreactivity were observed in RNFL, in some of the GCL cells, and in the inner nuclear layer. In contrast, no MT-like immunoreactivity was observed in the retina in MT-I/-II-deficient mice.

Activation of the NMDA receptor leads to an intracellular Ca^{2+} influx and to an increase in reactive oxygen species (ROS) that may be detrimental to cell viability.[30] Furthermore, activation of this receptor depletes intracellular GSH, which could decrease the intracellular capacity for inactivation of ROS.[31] Thus, oxidative stress, leading to the formation of ROS, has been implicated as a stage in the final common pathway for neurotoxicity in a wide variety of acute and chronic neurologic diseases such as stroke, Alzheimer's, and Parkinson's diseases. In such pathologic conditions, an increase in MT could compensate for the decreased radical-scavenging ability. Because we used an antibody that recognizes both MT-I and -II proteins in this study, we could not tell whether the increased MT-like immunoreactivity in the retina after NMDA injection represented MT-I or -II (or both). To clarify which MT isoform(s) might be increased after retinal damage, the time-course of the changes in the mRNA levels for MT isoforms (MT-I, -II, and -III) occurring after NMDA injection were examined in the retina of wild-type mice. The MT-II mRNA level was time-dependently elevated at 4 and 12 hours after NMDA injection, and it had returned to normal level by 24 hours (Fig. 2). In contrast, for MT-I and -III there were persistent decreases (to less than half control) from 4 to 24 hours. These findings suggest that the increased MT-like immunoreactivity we observed was derived from MT-II protein. In contrast, in studies of cerebral ischemia: (1) persistent increases in the expressions of MT-I and -II mRNA, but not of MT-III mRNA, in the infarcted cortex have been found after 72 hours cerebral ischemia reperfusion in mice and rats, and (2) increases in MT-I and -II mRNAs and MT protein have been detected in the endothelial cells of microvessels and in astrocytes in the infarcted cortex (by in situ hybridization and immunocytochemistry).[23,32] Our findings differ from these previous reports in that the MT-I mRNA level showed a persistent decrease in the retina after NMDA injection. This discrepancy may reflect differences in experimental conditions and/or in the target tissue examined.

To investigate the functional role of MT we used MT-I/-II-deficient mice, which have inactivated MT-I and -II genes.[33] Such mice possess a reduced radical-scavenging capability and an increased sensitivity to cadmium.[25,34] Furthermore, they have been reported to exhibit not only a poor neurologic outcome after stroke (versus wild-type animals), but also increased infarct volumes.[32] In the present study, the cell loss in GCL was significantly greater in MT-I/-II-deficient mice than in wild-type mice at 7 days after an intravitreous injection of NMDA (Fig. 3). In contrast, no significant difference in IPL thickness was observed between MT-I/-II-deficient and wild-type mice. These results seem consistent with our observations of marked increases in MT-like immunoreactivity in RNFL and in GCL cells, but not in IPL. Taken together, our results indicate that MT may exert an important neuroprotectant influence over retinal ganglion cells.

Next, we examined whether the upregulation of MT induced by zinc sulfate ($ZnSO_4$) or Vit. D_3 would protect against cell death in the NMDA-damaged retina in vivo and/or against

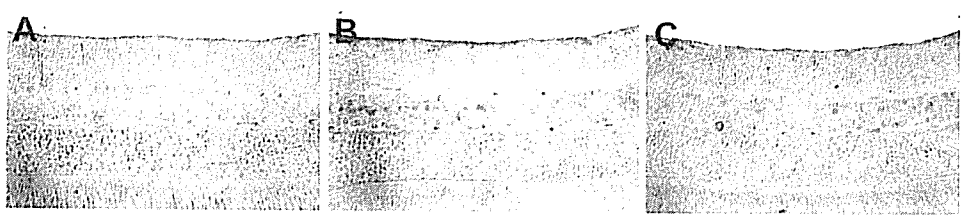

FIGURE 5. Effect of Vit. D_3 on MT-like immunoreactivity in mouse retina. Retinal cross sections were labeled with a primary antibody against MT in wild-type mice 24 hours after intravitreous injection of (A) vehicle, (B) Vit. D_3 (0.2 ng/eye: low dose), or (C) Vit. D_3 (2 ng/eye: high dose). Scale bar, 50 μm.

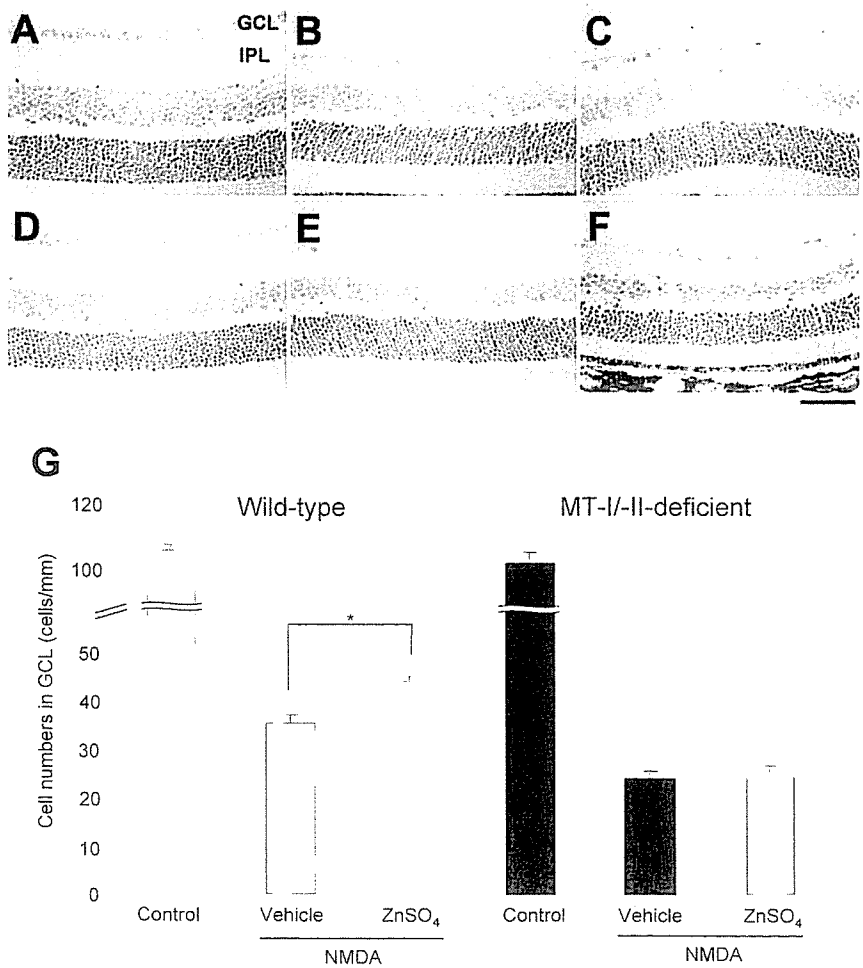

FIGURE 6. Effects of $ZnSO_4$ on retinal damage in MT-deficient or wild-type mice after NMDA injection. Retinal damage was evaluated in cross sections at 7 days after intravitreous injection of NMDA (40 nmol) in mice given either $ZnSO_4$ (10 nmol) or vehicle intravitreously at 24 hours before the NMDA injection. (**A**) Vehicle-treated control in wild-type mice, (**B**) NMDA+vehicle in wild-type mice, (**C**) NMDA+$ZnSO_4$ in wild-type mice, (**D**) vehicle-treated control in MT-deficient mice, (**E**) NMDA+vehicle in MT-deficient mice, and (**F**) NMDA+$ZnSO_4$ in MT-deficient mice. Scale bar, 50 μm. (**G**) The number of cells in the GCL from wild-type and MT-deficient mice. Data are the mean ± SEM of results in five to eight animals. $^*P < 0.05$ versus NMDA+vehicle in wild-type mice (Student's *t*-test).

oxidative stress-induced cell death in vitro. It has been reported that transcription of MT genes is upregulated in response to zinc,[35] and that oral administration of Vit. D_3 to mice results in increased levels of MT mRNA in the liver, kidney, and skin.[28] In our study, intravitreous injection of $ZnSO_4$ at 10 nmol/eye or of Vit. D_3 at 0.2 or 2 ng/eye in wild-type mice markedly elevated MT-like immunoreactivity in the inner retina, especially in RNFL and GCL cells. Moreover, pretreatment

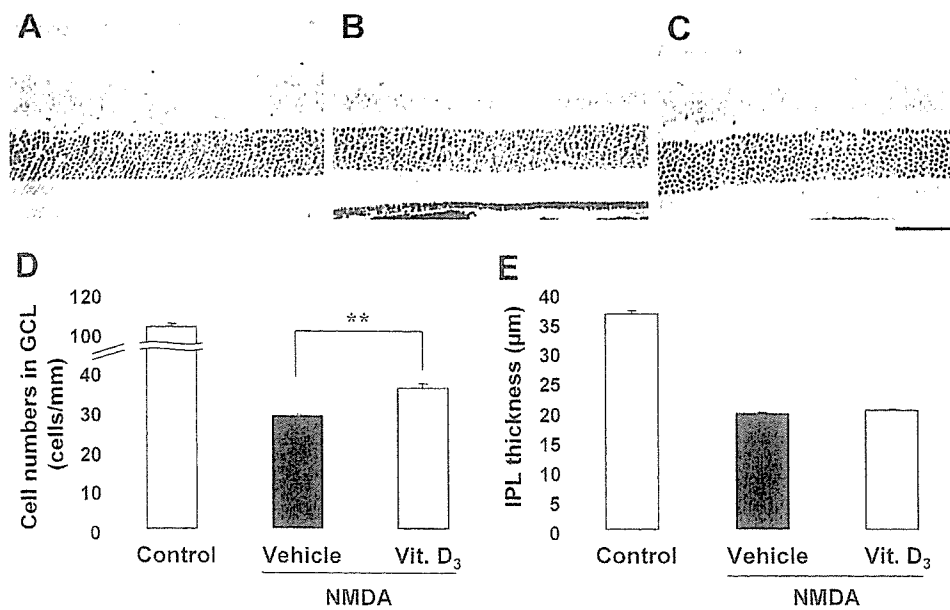

FIGURE 7. Effect of Vit. D_3 on retinal ganglion cell damage observed in wild-type mice after NMDA injection. Retinal cross sections were prepared 7 days after intravitreous injection of NMDA (40 nmol) in mice given either Vit. D_3 (2 ng) or vehicle intravitreously at 24 hours before the NMDA injection. (**A**) Control (nontreated control retina), (**B**) NMDA+vehicle-treated retina, (**C**) NMDA+Vit. D_3-treated retina. Scale bar, 50 μm. Retinal damage was evaluated by counting the number of cells in the GCL (**D**) and measuring the thickness of the IPL (**E**). Control (nontreated control group, □), NMDA+vehicle (▨), and NMDA+Vit. D_3 (■). Data are the mean ± SEM for 10 or 11 animals. $^{**}P < 0.01$ versus NMDA+vehicle-treated group (Student's *t*-test).

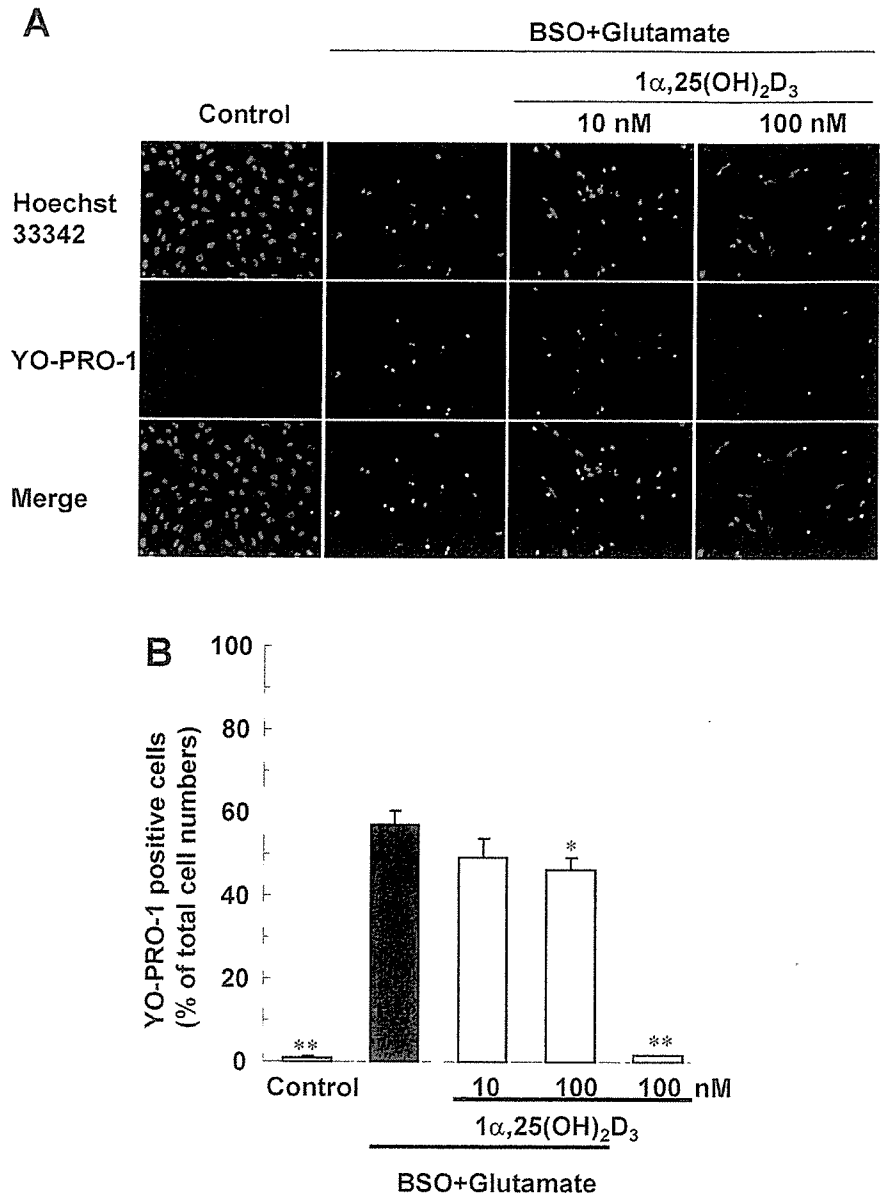

FIGURE 8. Effect of Vit. D_3 on RGC-5 death induced by oxidative stress in vitro. (**A**) Representative fluorescence microscopy showing nuclear staining for Hoechst 33342 (*blue*) and YO-PRO-1 (*green*) at 24 hours after BSO (500 μM)+glutamate (10 mM) treatment. One hour later, BSO with either glutamate or vehicle was added to each well. Viable cells were Hoechst 33342 -and YO-PRO-1-negative, whereas dead cells are Hoechst 33342 -and YO-PRO-1-positive. Vehicle-treated control cells showed normal nuclear morphology and were negatively stained for YO-PRO-1. BSO+glutamate-treated cells included YO-PRO-1-positive cells showing shrinkage and condensation of their nuclei. Pretreatment with Vit. D_3 at 100 nM reduced both nuclear shrinkage and YO-PRO-1-positive staining. (**B**) The number of cells exhibiting YO-PRO-1 fluorescence was counted, and positive cells were expressed as the ratio of YO-PRO-1- to Hoechst 33342-positive cells. Vit. D_3 treatment at 100 nM significantly inhibited the increase in YO-PRO-1-positive cells induced by BSO+glutamate. Data are the mean ± SEM (n = 8). $^*P < 0.05$, $^{**}P < 0.01$ versus BSO+glutamate alone (Student's t-test).

with $ZnSO_4$ protected against the cell loss in GCL induced by NMDA in wild-type mice, and this effect was not apparent in MT-I/-II-deficient mice (Fig. 6). However, in this study comparisons were based on small sample sizes in the different subgroups (n = 5-8)—a possible limitation of the study. Pretreatment with Vit. D_3 also showed evidence of protective effects in wild-type mice (Fig. 7). Previous studies[36,37] have found (1) that zinc pretreatment significantly reduces the increased levels of thiobarbituric acid-reactive substance (a marker of oxidative status) and of conjugated diene during ischemia-reperfusion and also increases metallothionein levels (versus saline injection), and (2) that Vit. D_3 inhibits oxygen-mediated ultraviolet injury in mouse skin indicating a protective effect of Vit. D_3 via induced MT. In the present experiment on RGC-5 in vitro, Vit. D_3 inhibited the oxidative stress-related cell death caused by depletion of GSH and inhibition of cystine uptake (induced by treatment with a combination of buthionine sulfoximine and glutamate; Fig. 8). Taken together, these findings suggest that the protective effects of $ZnSO_4$ and Vit D_3 may each be attributable to an upregulation of MT. However, we did not examine the effect of Vit D_3 in MT-I/-II-deficient mice in this study. Therefore, we could not exclude the possibility that the protective effect of Vit. D_3 is derived from other mechanisms, although MT protein was markedly increased in retina after the intravitreous injection of Vit. D_3.

In conclusion, we have demonstrated that MT-II mRNA is upregulated in the injured murine retina and that MT-I/-II knockdown exacerbates retinal damage. Hence, our findings suggest that MT, especially MT-II, plays a central role as a neuroprotectant against retinal neuronal damage.

Acknowledgments

The authors thank Yuta Inokuchi, Yasuhisa Oida, and Nobutaka Morimoto (Department of Biofunctional Molecules, Gifu Pharmaceutical University, Gifu, Japan) for skillful technical assistance.

References

1. Dreyer EB, Zurakowski D, Schumer RA, et al. Elevated glutamate levels in the vitreous body of humans and monkeys with glaucoma. *Arch Ophthalmol.* 1996;114:299-305.

2. Dreyer EB. A proposed role for excitotoxicity in glaucoma. *J Glaucoma.* 1998;7:62-67.
3. Bonfoco E, Krainc D, Ankarcrona M, et al. Apoptosis and necrosis: two distinct events induced, respectively, by mild and intense insults with N-methyl-D-aspartate or nitric oxide/superoxide in cortical cell cultures. *Proc Natl Acad Sci USA.* 1995;92:7162-7166.
4. Bastianetto S, Quirion R. Natural antioxidants and neurodegenerative diseases. *Front Biosci.* 2004;9:3447-3452.
5. Selim MH, Ratan RR. The role of iron neurotoxicity in ischemic stroke. *Ageing Res Rev.* 2004;3:345-353.
6. HaMai D, Bondy SC. Oxidative basis of manganese neurotoxicity. *Ann N Y Acad Sci.* 2004;1012:129-141.
7. Townsend DM, Tew KD, Tapiero H. The importance of glutathione in human disease. *Biomed Pharmacother.* 2003;57:145-155.
8. Pompella A, Visvikis A, Paolicchi A, et al. The changing faces of glutathione, a cellular protagonist. *Biochem Pharmacol.* 2003;66:1499-1503.
9. Harding JJ. Free and protein-bound glutathione in normal and cataractous human lenses. *Biochem J.* 1970;117:957-960.
10. Donma O, Yorulmaz E, Pekel H, Suyugul N. Blood and lens lipid peroxidation and antioxidant status in normal individuals, senile and diabetic cataractous patients. *Curr Eye Res.* 2002;25:9-16.
11. Gherghel D, Griffiths HR, Hilton EJ, et al. Systemic reduction in glutathione levels occurs in patients with primary open-angle glaucoma. *Invest Ophthalmol Vis Sci.* 2005;46:877-883.
12. Cicik E, Tekin H, Akar S, et al. Interleukin-8, nitric oxide and glutathione status in proliferative vitreoretinopathy and proliferative diabetic retinopathy. *Ophthalmic Res.* 2003;35:251-255.
13. Nowak M, Swietochowska E, Wielkoszynski T, et al. Changes in blood antioxidants and several lipid peroxidation products in women with age-related macular degeneration. *Eur J Ophthalmol.* 2003;13:281-286.
14. Kagi JH, Vallee BL. Metallothionein: a cadmium and zinc-containig protein from equine renal cortex. II Physico-chemical properties. *J Biol Chem.* 1961;236:2435-2442.
15. Klaassen CD, Lehman-McKeeman LD. Regulation of the isoforms of metallothionein. *Biol Trace Elem Res.* 1989;21:119-129.
16. Hidalgo J, Dingman A, Garvey JS. Preparative isolation of adult human liver metallothionein isoforms. *Rev Esp Fisiol.* 1989;45:255-263.
17. Palmiter RD, Findley SD, Whitmore TE, Durnam DM. MT-III, a brain-specific member of the metallothionein gene family. *Proc Natl Acad Sci USA.* 1992;89:6333-6337
18. Vasak M. Advances in metallothionein structure and functions. *J Trace Elem Med Biol.* 2005;19:13-17
19. Thornalley PJ, Vasak M. Possible role for metallothionein in protection against radiation-induced oxidative stress: kinetics and mechanism of its reaction with superoxide and hydroxyl radicals. *Biochim Biophys Acta.* 1985;827:36-44.
20. Bremner I. Nutritional and physiologic significance of metallothionein. *Methods Enzymol.* 1991;205:25-35.
21. Hamer DH. Metallothionein. *Annu Rev Biochem.* 1986;55:913-951.
22. Dunn MA, Blalock TL, Cousins RJ. Metallothionein. *Proc Soc Exp Biol Med.* 1987;185:107-119.
23. Campagne MV, Thibodeaux H, van Bruggen N, et al. Increased binding activity at an antioxidant-responsive element in the metallothionein-1 promoter and rapid induction of metallothionein-1 and -2 in response to cerebral ischemia and reperfusion. *J Neurosci.* 2000;20:5200-5207.
24. van Lookeren Campagne M, Thibodeaux H, van Bruggen N, et al. Evidence for a protective role of metallothionein-1 in focal cerebral ischemia. *Proc Natl Acad Sci USA.* 1999;96:12870-12875.
25. Masters BA, Kelly EJ, Quaife CJ, et al. Targeted disruption of metallothionein I and II genes increases sensitivity to cadmium. *Proc Natl Acad Sci USA.* 1994;91:584-588.
26. Shimazawa M, Yamashima T, Agarwal N, Hara H. Neuroprotective effects of minocycline against in vitro and in vivo retinal ganglion cell damage. *Brain Res.* 2005;1053:185-194.
27. Kramer KK, Zoelle JT, Klaassen CD. Induction of metallothionein mRNA and protein in primary murine neuron cultures. *Toxicol Appl Pharmacol.* 1996;141:1-7.
28. Karasawa M, Hosoi J, Hashiba H, et al. Regulation of metallothionein gene expression by 1 alpha,25-dihydroxyvitamin D3 in cultured cells and in mice. *Proc Natl Acad Sci USA.* 1987;84:8810-8813.
29. Maher P, Hanneken A. The molecular basis of oxidative stress-induced cell death in an immortalized retinal ganglion cell line. *Invest Ophthalmol Vis Sci.* 2005;46:749-757.
30. Choi DW. Excitotoxic cell death. *J Neurobiol.* 1992;23:1261-1276.
31. Wallin C, Weber SG, Sandberg M. Glutathione efflux induced by NMDA and kainate: implications in neurotoxicity? *J Neurochem.* 1999;73:1566-1572.
32. Trendelenburg G, Prass K, Priller J, et al. Serial analysis of gene expression identifies metallothionein-II as major neuroprotective gene in mouse focal cerebral ischemia. *J Neurosci.* 2002;22:5879-5888.
33. Michalska AE, Choo KH. Targeting and germ-line transmission of a null mutation at the metallothionein I and II loci in mouse. *Proc Natl Acad Sci USA.* 1993;90:8088-8092.
34. Sato M, Bremner I. Oxygen free radicals and metallothionein. *Free Radic Biol Med.* 1993;14:325-337.
35. Andrews GK. Regulation of metallothionein gene expression by oxidative stress and metal ions. *Biochem Pharmacol.* 2000;59:95-104.
36. Ogawa T, Mimura Y. Antioxidant effect of zinc on acute renal failure induced by ischemia-reperfusion injury in rats. *Am J Nephrol.* 1999;19:609-614.
37. Hanada K, Sawamura D, Nakano H, Hashimoto I. Possible role of 1,25-dihydroxyvitamin D3-induced metallothionein in photoprotection against UVB injury in mouse skin and cultured rat keratinocytes. *J Dermatol Sci.* 1995;9:203-208.

Jpn J Ophthalmol 2006;50:449–454

DOI 10.1007/s10384-006-0343-z

CLINICAL INVESTIGATION

Diurnal Variation of Intraocular Pressure in Suspected Normal-Tension Glaucoma

Kou Hasegawa, Kyoko Ishida, Akira Sawada, Kazuhide Kawase, and Tetsuya Yamamoto

Department of Ophthalmology, Gifu University Graduate School of Medicine, Gifu, Japan

Abstract

Purpose: To assess diurnal variations of intraocular pressure (IOP) in suspected normal-tension glaucoma (NTG) patients with subsequent long-term observation to detect changes that may lead to a new diagnosis.

Methods: Diurnal variation of IOP was measured in a sitting position at 2-h intervals for 24 h in a total of 569 subjects with suspected NTG.

Results: Thirty of the 569 subjects (5.3%) showed IOP values exceeding 20 mmHg during the 24-h monitoring and were diagnosed as having primary open-angle glaucoma (POAG). In subjects in whom NTG was definitely diagnosed based on the results of the 24-h monitoring, the average maximum, minimum, and mean IOP was 16.1, 11.7, and 13.9 mmHg, respectively, and the mean diurnal variation in IOP was 4.4 mmHg. The peak time was observed outside clinic hours (1800–0800) in 41.4% of patients, and the trough time was observed during clinic hours (1000–1600) in 15.9%. In 2.9% of NTG subjects, the diagnosis was eventually changed to POAG during follow-up.

Conclusion: Assessment of diurnal variations of IOP in suspected NTG patients is useful for the differential diagnosis of POAG from NTG and for establishment of a baseline, which may affect the management plan. **Jpn J Ophthalmol** 2006;50:449–454 © Japanese Ophthalmological Society 2006

Key Words: diurnal variations, intraocular pressure, normal-tension glaucoma

Introduction

Normal-tension glaucoma (NTG) is defined as "glaucomatous optic neuropathy in which the intraocular pressure (IOP) remains always in the statistically determined normal range during the course of onset and progression,"[1] and it is regarded as a subtype of primary open-angle glaucoma (POAG) in the broad sense of the term. In addition to IOP, multiple factors such as papillary/peripapillary circulatory disorders and autoimmune abnormalities are thought to be involved in the onset of optic nerve disorders in NTG. From the clinical viewpoint, however, IOP is considered to play the greatest role in optic nerve disorders in NTG.[2–5] It is widely accepted that IOP reduction is the only clinically reliable means of suppressing the progression of visual field loss.[2–5]

Since Maslenikow[6] first reported in 1904 that "IOP shows diurnal variations," based on tonometer results, numerous subsequent studies have documented this phenomenon. IOP is reported to be generally higher in the morning and lower in the evening, and this variation has been classified into several types. On the basis of past reports, Katavisto[7] divided diurnal variation patterns into a regular type, which resembled a biorhythm, and an irregular type, with no such resemblance, and further subdivided the regular type into three subtypes: morning, day, and night types.

According to an epidemiological study carried out by the Japan Glaucoma Society in Tajimi in 2000–2001 (the Tajimi Study),[8] the prevalence of POAG (in the narrow sense of the term) in Japanese people aged ≥40 years was reported as 0.3%, and the prevalence of NTG was 3.6%, indicating an extremely high ratio of NTG to POAG. It is thus helpful

Received: December 20, 2005 / Accepted: March 24, 2006
Correspondence and reprint requests to: Kou Hasegawa, Department of Ophthalmology, Gifu University Graduate School of Medicine, 1-1 Yanagido, Gifu 501-1194, Japan

Jpn J Ophthalmol
Vol 50: 449–454, 2006

to assess IOP in Japanese NTG patients, because diurnal variations of IOP are extremely useful for assessing disease status and for designing treatment plans. In this retrospective study, we determined the diurnal variations of IOP at a single medical institution in over 500 nonmedicated subjects with suspected NTG. We report the features of the diurnal variations of IOP in subjects diagnosed as having NTG and in those in which the diagnosis was changed to POAG during long-term follow-up.

Subjects and Methods

The subjects were 569 Japanese patients (1138 eyes) who attended the glaucoma clinic of the Gifu University Hospital, Gifu, Japan, between January 1989 and December 2003 and who had completed the following diurnal IOP measurement series because of suspected NTG. The diurnal variation of IOP was measured before the start of treatment with antiglaucoma medication, or at least 4 weeks after the antiglaucoma medication was washed out. The study group comprised 237 men and 332 women, aged 57.8 ± 12.9 years (mean ± standard deviation; range, 15–86 years). The criteria for suspected NTG were (1) an IOP chronically ≤20 mmHg in both eyes, irrespective of the presence or absence of treatment; (2) a normal open angle (grade 3 or 4 according to Shaffer's classification); (3) the presence of a glaucomatous optic nerve change (a cup/disc ratio of ≥0.7, thinning of the disc rim, retinal nerve fiber layer defect, or a difference of ≥0.2 in the cup/disc ratio between the left and right eyes); (4) the presence of a corresponding glaucomatous visual field change in the full-threshold central 30–2 program using a Humphrey Field Analyzer (HFA, model 740; Carl Zeiss Meditec, Dublin, CA, USA); and (5) the absence of an intraocular or intracranial lesion affecting the optic nerve or visual field, which were examined with computed tomography and magnetic resonance imaging. All subjects had fulfilled the NTG criteria shown above. Subjects with a history of surgery (including laser surgery) such as for cataract or glaucoma were excluded from this study. The IOP was determined at 2-h intervals from 1000 to 0800 the next morning, for a total of 12 measurements taken by a Goldmann applanation tonometer. IOP was measured at each time point with the same tonometer, with the patient in a sitting position. When asleep at night, the subject was awakened by gently touching the shoulder, and the position change and assessment of IOP were completed within 5 min. Each subject was assessed with the same tonometer. The IOP measurement was taken three times at each time point by experienced physicians; however, the same subject might have been assessed, in a masked fashion, by different physicians depending upon the time of the assessment. The procedure for measuring diurnal variation of IOP was explained in advance to all subjects. In subjects with suspected NTG, we diagnosed primary open-angle glaucoma (POAG) if an IOP value exceeding 20 mmHg in at least one eye was found during the 24-h assessment period. Subjects whose IOP values were chronically ≤20 mmHg in both eyes throughout the 24-h assessment period were diagnosed as having NTG.

In subjects diagnosed as having NTG, the diurnal variation pattern of IOP was analyzed. Subjects with NTG and with pseudoexfoliative materials (PE materials) were excluded from subsequent analysis. The time point of maximum IOP during the day was defined as the "peak time," and the time point of minimum IOP was defined as the "trough time." When a peak was observed at least twice, the sum of the values observed before and after the time point were compared and the time point at which the sum was highest was defined as the peak time. When a trough was observed at least twice, the sum of the values observed before and after the time point were compared and the time point at which the sum was lowest was defined as the trough time. Subjects in whom it was difficult to identify a peak time or trough time as a single time point were excluded from the analysis. In subjects for whom the peak time and trough time could be identified in both eyes, we determined whether the peak time or trough time was coincident in the two eyes.

When an IOP value of >20 mmHg was noted twice during follow-up under no treatment, or during treatment with medication in subjects in whom NTG was diagnosed after completing the assessment of the diurnal variation of IOP, a change of diagnosis to POAG was made, and the period from completing the assessment of the diurnal variation of IOP to the change of diagnosis to POAG was determined. The follow-up period continued until the end of December 2004, and the subjects were then divided into three groups, depending on the time period from completing the assessment of the diurnal variation of IOP to the change of diagnosis to POAG, as follows: ≤1 year, from 1 to 5 years, and >5 years.

Results

Of the 569 subjects in whom the 24-h measurements were completed, 30 (5.3%) showed an IOP value exceeding 20 mmHg in at least one eye, and were thus diagnosed as having POAG. Thirteen of the 30 POAG subjects (43.3%) showed an IOP value that exceeded 20 mmHg between 1800 and 0800, which was outside the clinic hours (clinic hours, 1000 to 1600). The remaining 539 subjects were diagnosed as having NTG. Of the 539 subjects in whom NTG was diagnosed, PE materials were recognized in 15 subjects (2.6%), and these subjects were excluded from further evaluation in this study.

The remaining 524 subjects (1048 eyes), who were definitely diagnosed as having NTG without PE material, comprised 218 men and 306 women aged 57.5 ± 12.8 years (mean ± SD, range 15–85 years), with 94.6% being ≥40 years old. The mean refraction value (equivalent spherical value) was −2.5 ± 4.0 D (−20.0 to +5.5 D): 317 eyes (30.2%) were emmetropic or hypermetropic with a refraction value of ≥0 D; 521 eyes (49.8%) were mildly or moderately myopic with a refraction value of ≥−6 D and <0 D; and 210 eyes

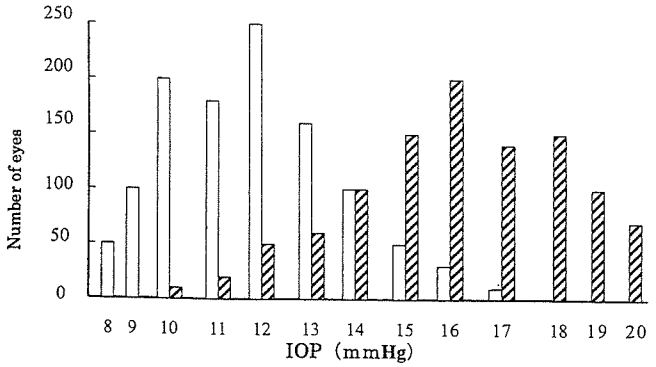

Figure 1. Maximum and minimum intraocular pressure (*IOP*) at 12 measurement times in 524 subjects with normal-tension glaucoma (NTG). *Striped columns*, maximum IOP; *open columns*, minimum IOP.

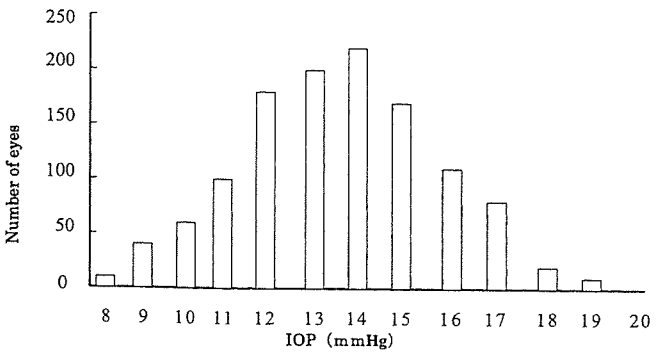

Figure 2. Mean IOP at 12 measurement times in 524 subjects with NTG.

(20.0%) were severely myopic with a refraction value of <–6D. The mean deviation (MD) was –9.02 ± 7.30dB (–34.03 to +2.63dB), and the MD values were classified by severity according to Anderson's classification:[9] 460 eyes (44.1%) were early stage (MD > –6dB); 270 eyes (25.8%) were middle stage (–12dB ≤ MD ≤ –6dB); and 315 eyes (30.1%) were late stage (MD < –12dB).

Figure 1 shows the maximum and minimum IOP values. Among the 524 subjects (1048 eyes) who were definitely diagnosed as having NTG without PE materials, the maximum IOP was 16.1 ± 2.2mmHg (10–20mmHg) and the minimum IOP was 11.7 ± 2.1mmHg (8–17mmHg). Figure 2 shows mean IOP values. The mean IOP was 13.9 ± 2.0mmHg (8.3–19.1mmHg), and the mean difference in IOP between a patient's two eyes (absolute value) was 0.50 ± 0.50mmHg (0–2.6mmHg). The difference between eyes was relatively small, ≤2mmHg, in 97.7% of the NTG subjects.

Among the 524 subjects (1048 eyes) who were definitely diagnosed as having NTG with an absence of PE materials, the mean diurnal variation of IOP was 4.4 ± 1.6mmHg (1–10mmHg): 607 eyes (57.9%) had a variation of ≤4mmHg, and 256 eyes (24.4%) had a variation of ≥6mmHg (Fig. 3). A peak time and trough time were identified in 507 subjects (970 eyes) among the 524 subjects

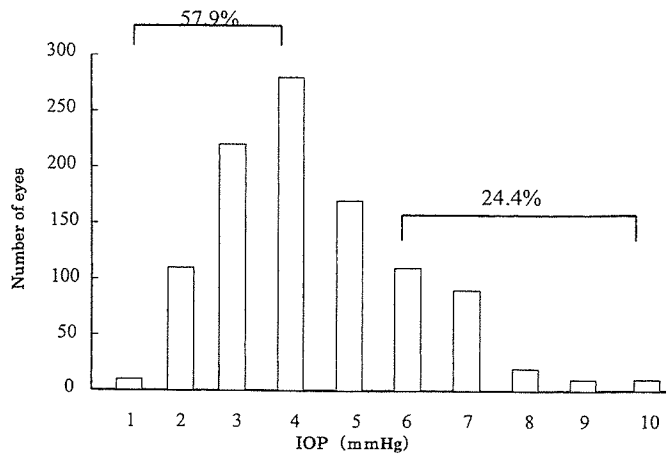

Figure 3. Mean diurnal variation of IOP at 12 measurement times in 524 subjects with NTG.

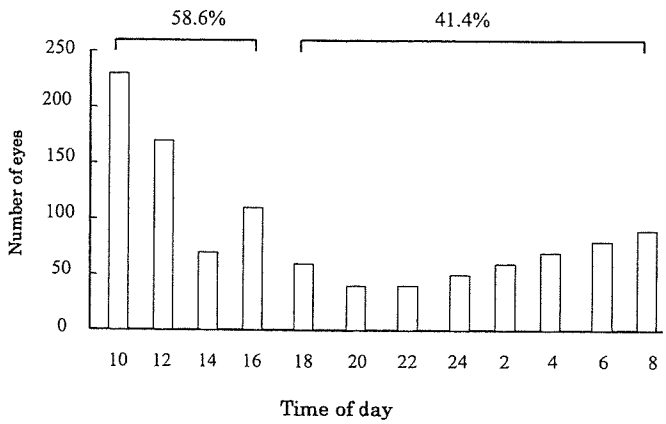

Figure 4. Peak time in 507 of 524 NTG subjects.

(1048 eyes). The peak time was identified as 1000, 1200, 1600, and 1400 in 23.0%, 16.7%, 11.2%, and 7.7% of subjects, respectively: 58.6% of subjects showed a peak during clinic hours (1000–1600), and 41.4% of subjects showed a peak outside clinic hours (Fig. 4). Highly significant correlations were noted between the peak IOP and the IOP at 1000 ($r = 0.752$, $P < 0.001$), the IOP at 1200 ($r = 0.771$, $P < 0.001$), the IOP at 1400 ($r = 0.760$, $P < 0.001$), and the IOP at 1600 ($r = 0.769$, $P < 0.001$). The trough time was identified as 0000, 0200, 0400, and 2200 in 18.0%, 13.4%, 13.2%, and 12.6% of subjects, respectively. In 15.9% of subject s, the trough time was observed during clinic hours (Fig. 5). Highly significant correlations were noted between the trough IOP and the IOP at 2200 ($r = 0.787$, $P < 0.001$), the IOP at 0000 ($r = 0.779$, $P < 0.001$), the IOP at 0200 ($r = 0.784$, $P < 0.001$), and the IOP at 0400 ($r = 0.772$, $P < 0.001$). If a left/right difference of ≤2h was regarded as coincidence, then among the 463 subjects in whom both the peak time and trough time could be identified for both eyes, coincidence was seen in both the peak time and trough time in 341 subjects (73.7%), in the peak time only in 44 subjects

Jpn J Ophthalmol
Vol 50: 449–454, 2006

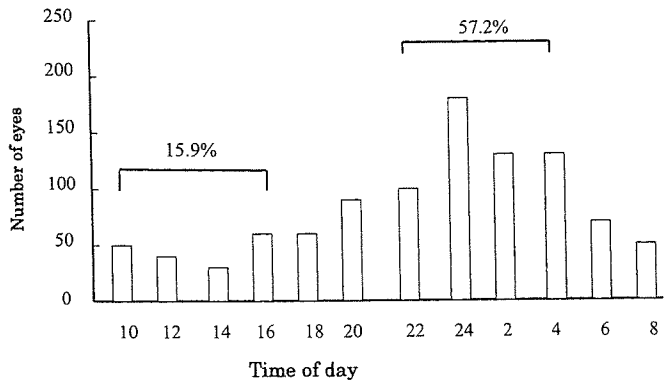

Figure 5. Trough time in 507 of 524 NTG subjects.

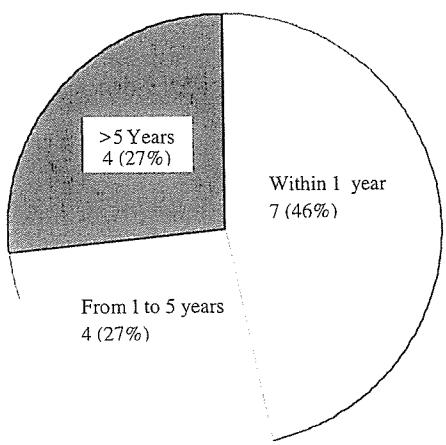

Figure 6. The follow-up period until change of diagnosis to primary open-angle glaucoma in subjects with NTG.

(9.5%), and in the trough time only in 57 subjects (12.3%). Coincidence was not seen in either the peak time or the trough time in 21 subjects (4.5%).

Among the 524 subjects who were definitely diagnosed as having NTG without PE materials, the diagnosis was changed to POAG because of an increase in IOP in 15 subjects during follow-up. The time period from completion of the assessment of the diurnal variation of IOP to the change of diagnosis to POAG was ≤1 year in seven subjects (46%), from 1 to 5 years in four subjects (27%), and >5 years in four subjects (27%) (Fig. 6).

Discussion

According to an epidemiological study carried out by the Japan Glaucoma Society in Tajimi in 2000–2001 (the Tajimi Study),[8] the prevalence of POAG (in the wide sense of the term) was 3.9% in Japanese people aged ≥40 years, which was higher than that in Chinese people living in Singapore,[10] and close to that in black populations.[11–13] In the Tajimi Study,[8] the prevalence of POAG (in the wide sense of the term) was 3.9%, and the prevalence of NTG was 3.6%; thus, 92% of the POAG cases were classified as NTG in Japanese people. Most of the studies on diurnal variations of IOP in NTG subjects taking no medication have been performed in Japanese populations, except for a study by Sacca et al.[14] Only two studies, those by Yamagami et al.[15] and Kano and Kuwayama,[16] have measured diurnal variations using study groups of more than 100 NTG subjects. The present study was the first to assess diurnal variations in over 500 patients at a single medical institution, and we focused on the diurnal variations of IOP in subjects with suspected NTG who were not being medicated. Our results showed an average maximum IOP of 16.1 ± 2.2 mmHg, an average minimum IOP of 11.7 ± 2.1 mmHg, an average mean IOP of 13.9 ± 2.0 mmHg, and an average diurnal variation of 4.4 ± 1.6 mmHg. In previous studies of diurnal variations of IOP in Japanese NTG subjects, the average maximum IOP was reported as 16.5–16.8 mmHg, the average minimum IOP was 11.8–12.8 mmHg, the average mean IOP was 14.1–14.8 mmHg, and the average diurnal variation was 4.0–4.8 mmHg.[15,16] It has been reported that the maximum IOP in healthy Japanese subjects in whom the IOP was measured at 1-h intervals is 17.0–17.4 mmHg, the minimum IOP is 10.5–10.9 mmHg, and the diurnal variation is 6.5 mmHg.[17,18] We cannot explain fully why the diurnal variation of IOP in healthy normal eyes in those studies[17,18] exceeded that of the present study, but we speculate that the difference in measurement intervals may explain it partly. In the present study, the minimum IOP and diurnal variation of IOP were consistent with previous data, but the maximum IOP was slightly lower; consequently, the mean IOP was also slightly lower. The variation of IOP was ≤4 mmHg in 57.9% of subjects, and was ≥6 mmHg in 24.4% of subjects. Kano and Kuwayama[16] found that 10.3% of subjects with NTG had a variation of IOP ≥6 mmHg, measured with home tonometers. In the present study, the variation was as great as 10 mmHg in two subjects (three eyes). These results suggest that in some NTG patients, variations of IOP may be large and not recognized during clinic hours; thus, the baseline IOP may be mistakenly assessed if IOP is measured during clinic hours only.

The typical pattern of IOP variation seen in the present study, in which the peak time occurred between the morning and early afternoon and the trough time occurred between afternoon and night, was similar to the pattern previously reported in healthy subjects and in patients with ocular hypertension, POAG, or NTG.[15–18] Horie and Kitazawa[18] examined 186 eyes in healthy subjects and glaucoma or ocular hypertensive patients and found a positive correlation between the peak IOP and the IOP at 1100 or 1200, and also between the trough IOP and the IOP at 0000 or 0200. In the present study of 524 NTG subjects, a positive correlation was seen between the peak IOP and the IOP at 1000, 1200, 1400, and 1600, and also between the trough IOP and the IOP at 2200, 0000, 0200, and 0400. The peak time was seen more frequently at 1000 (23.0%), 1200 (16.7%), 1600 (11.2%), and 1400 (7.7%), and the trough time was more frequent at 0000 (18.0%), 0200 (13.4%), 0400 (13.2%), and 2200 (12.6%). However, 41.4% of subjects in the

present study had a peak time outside clinic hours, and 15.9% showed a trough time during clinic hours. Thus, overall IOP might be underestimated if measured only during clinic hours.

Even in patients in whom NTG is diagnosed by assessment of diurnal variations of IOP, this diagnosis is subject to change during a long-term follow-up. Previous epidemiological surveys of glaucoma have revealed a negative correlation between IOP and age in healthy Japanese subjects.[19] However, Shiose et al.[19] reported that in 11.7% of Japanese subjects in whom NTG was diagnosed by measurement of IOP, the diagnosis was changed to POAG within the next year based on an increase in IOP. In the present study, among the 524 subjects in whom NTG was diagnosed with an assessment of the diurnal variations of IOP, a change of diagnosis to POAG was made in 15 (2.9%) subjects because of an increase in IOP observed during follow-up. In the epidemiological study of Shiose et al.,[19] the IOP values used for the diagnosis of NTG were obtained at a single examination, and no assessments of the diurnal variations of IOP were made. Clearly, an assessment of the diurnal variations of IOP can improve the precision of diagnosis in glaucoma. In the current study, a change of diagnosis to POAG was made within 1 year of follow-up in 7 (46 %), from 1 to 5 years in 4 (27%), and after >5 years in 4 (27%) of the 15 subjects. However, the follow-up period ranged from 1 to 15 years, and further changes in diagnosis might be expected with a longer follow-up.

IOP is known to vary simultaneously in the left and right eyes, and this includes diurnal variations. Kitazawa and Horie[17] and Horie and Kitazawa[18] reported that both eyes in the same subject showed almost parallel changes in IOP irrespective of the presence of glaucoma. In the present study, both eyes were assessed to investigate the pattern of diurnal variation as well as the coincidence rate between the left and right eyes. In subjects in whom the peak time and trough time could be identified for both eyes, we found a 73.7% coincidence rate in subjects in whom the time differences in the peak time and trough time between the left and right eyes were ≤2 h, which was markedly higher than the 50.4% rate reported by Kano and Kuwayama[16] for IOP measured with home tonometers.

The difference in IOP between both eyes is reported to be ≤2 mmHg in 92.9%–93.2% of healthy subjects,[17,18] and in the present study we found that 97.7% of the subjects had a difference of ≤2 mmHg. This suggests that the difference in the IOP between left and right eyes in NTG is similar to that of healthy subjects.

Our measurements of the diurnal variations of IOP were taken with the patient in sitting position during hospitalization, as described elsewhere,[15,17,18] and we recognize that this is an unfamiliar and potentially disturbing environment for subjects, which could confound the measurement of the natural variation pattern of IOP. Yet hospitalization also allowed precise control of the measurement method and timing and the use of physicians as data collectors. Liu et al.[20–23] measured IOP in the sitting position during the day and in a supine position at night under strict control in a sleep laboratory. They found that an IOP trough occurred just before the subjects had lain down and fallen asleep and that a significantly higher IOP occurred during sleep in a supine position compared with the IOP measured while the subject was sitting up before going to sleep or after awaking. It is desirable to determine IOP in postures corresponding to daily activities, but since it is difficult to access ideal facilities, such as a sleep laboratory, we sought to minimize the confounding effect of posture by a comparison with past studies in which IOP was determined in the sitting position. Although other studies[16,24] have noted the drawbacks of inpatient assessment, such as high cost, disturbance of the patient's daily routine, and hospital-related restrictions on timing, and have experimented with a prototype self-measuring noncontact air-puff tonometer (home tonometer), which can be used by patients in their normal environment, a Goldmann applanation tonometer is still considered to give greater precision and has remained the clinical standard for the care of glaucoma patients. It should also be noted that, in the present study, different physicians used the same Goldmann tonometer for the same subject at different measurement time points in masked fashion, although all were glaucoma specialists who were familiar with the use of this tonometer, and the measurements were sufficiently consistent among these physicians.

Diurnal variations of IOP are thought to be caused by changes in the production of aqueous humor under the influence of the sympathetic nervous system,[25,26] and IOP measurement may itself disturb the subject's autonomic nervous system through assessment-related stress or simple disruption of the daily routine. When interpreting results, it should be remembered that the IOP tends to be lower when subjects are assessed as inpatients rather than as outpatients,[27] that the IOP shows seasonal variations and tends to be higher in winter,[28,29] that there are problems in the reproducibility of diurnal variation patterns of IOP,[18,24] that IOP shows a transient increase following light stimulation,[21] that IOP varies according to the quality of sleep, and that IOP is lower during rapid eye movement sleep and higher during slow-wave sleep.[30]

In an epidemiological study, Leydhecker et al.[31] calculated the upper limit of the normal IOP range to be 21 mmHg (mean ± SD × 2), on the basis of an IOP of 15.5 ± 2.57 mmHg (mean ± SD), measured with a Schiotz tonometer. When the upper limit of the normal IOP range is calculated as described above, it is found to be 20.0 mmHg for the IOP value of 14.5 ± 2.5 mmHg (right eyes) obtained in the Tajimi Study.[8] On the basis of this value, we set the upper limit of the normal IOP range at 20 mmHg at our medical institution, which is 1 mmHg lower than the conventional value.

Because we set the upper limit value at 20 mmHg in our assessment of the diurnal variations of IOP, the proportion of subjects in whom POAG was diagnosed was 5.3% (30 of 569), in contrast to the 3.5% reported by Yamagami et al.[15] When the upper limit was set at 21 mmHg, 2.6% (15 of 569) were diagnosed as having POAG, a result slightly lower than that of Yamagami et al.[15] Of the subjects in whom the diag-

nosis was changed to POAG by assessment of the diurnal variations of IOP, 13 (43.3%) of 30 were so diagnosed based on raised IOP values that were detected only outside of clinic hours; thus, POAG was diagnosed in approximately 40% of subjects by determining the IOP outside of clinic hours, which underscores the value of measuring IOP outside of clinic hours.

In the present study, we assessed the diurnal variations of IOP in a large number of subjects with NTG without medication at our institution, and studied the characteristics of the diurnal variations. Our findings suggest that the measurement of the diurnal variations of IOP is useful not only for the differential diagnosis of POAG from NTG but also for assessing disease status and establishing a treatment plan.

References

1. Japan Glaucoma Society. Guidelines for glaucoma. 2004: Tokyo, Japan. http://www.rkokunaisho.jp
2. Araie M, Sekine M, Suzuki Y, Koseki N. Factors contributing to the progression of visual field damage in eyes with normal-tension glaucoma. Ophthalmology 1994;101:1440–1444.
3. Collaborative Normal-Tension Glaucoma Study Group. Comparison of glaucomatous progression between untreated patients with normal-tension glaucoma and patients with therapeutically reduced intraocular pressures. Am J Ophthalmol 1998;126:487–497.
4. Collaborative Normal-Tension Glaucoma Study Group. The effectiveness of intraocular pressure reduction in the treatment of normal tension glaucoma. Am J Ophthalmol 1998;126:498–505.
5. The AGIS Investigators. The advanced glaucoma intervention study (AGIS). 7. The relationship between control of intraocular pressure and visual field deterioration. Am J Ophthalmol 2000;130: 429–440.
6. Maslenikow AZ. Über Tagesschwankungen des intraokularen Druckes bei. Glaukom Augenheilk 1904;11:564.
7. Katavisto M. The diurnal variations of ocular tension in glaucoma. Acta Ophthalmol Suppl 1964;78:57–64.
8. Iwase A, Suzuki Y, Araie M, et al. The prevalence of primary open-angle glaucoma in Japanese: the Tajimi study. Ophthalmology 2004;111:1641–1648.
9. Anderson DR, Patella VM. Automated static perimetry. Mosby: St Louis; 1999.
10. Foster PJ, Oen FTS, Machin D, et al. The prevalence of glaucoma in Chinese residents of Singapore. A cross-sectional population survey of the Tanjong Pagar district. Arch Ophthalmol 2000;118: 1105–1111.
11. Buhrmann RR, Quigley HA, Barron Y, West SK, Oliva MS, Mmbaga BBO. Prevalence of glaucoma in a rural East African population. Invest Ophthalmol Vis Sci 2000;41:40–48.
12. Tielsch JM, Sommer A, Katz J, Royall RM, Quigley HA, Javitt J. Racial variations in the prevalence of primary open-angle glaucoma. The Baltimore Eye Survey. JAMA 1991;266:369–374.
13. Mason RP, Kosoko O, Wilson MR, et al. National survey of the prevalence and risk factors of glaucoma in St. Lucia, West Indies. Part 1. Prevalence findings. Ophthalmology 1989;96:1363–1368.
14. Sacca SC, Rolando M, Marletta A, Macri A, Cerqueti P, Ciurlo G. Fluctuations of intraocular pressure during the day in open-angle glaucoma, normal-tension glaucoma and normal subjects. Ophthalmologica 1998;212:115–119.
15. Yamagami J, Araie M, Aihara M, Yamamoto S. Diurnal variation in intraocular pressure of normal-tension glaucoma eyes. Ophthalmology 1993;100:643–650.
16. Kano K, Kuwayama Y. Diurnal variation of intraocular pressure in normal-tension glaucoma. Nippon Ganka Gakkai Zasshi (J Jpn Ophthalmol Soc) 2003;107:375–379.
17. Kitazawa Y, Horie T. Diurnal variation of intraocular pressure in primary open-angle glaucoma. Am J Ophthalmol 1975;79:557–566.
18. Horie T, Kitazawa Y. The clinical significance of diurnal pressure variation in primary open-angle glaucoma. Jpn J Ophthalmol 1979; 23:310–333.
19. Shiose Y, Kitazawa Y, Tsukahara S, et al. Epidemiology of glaucoma in Japan—a nationwide glaucoma survey. Jpn J Ophthalmol 1991;35:133–155.
20. Liu JHK, Kripke DF, Hoffman RE, et al. Nocturnal elevation of intraocular pressure in young adults. Invest Ophthalmol Vis Sci 1998;39:2707–2712.
21. Liu JHK, Kripke DF, Hoffman RE, et al. Elevation of human intraocular pressure at night under moderate illumination. Invest Ophthalmol Vis Sci 1999;40:2439–2442.
22. Liu JHK, Kripke DF, Twa MD, et al. Twenty-four-hour pattern of intraocular pressure in the aging population. Invest Ophthalmol Vis Sci 1999;40:2912–2917.
23. Liu JHK, Zhang X, Kripke DF, Weinreb RN. Twenty-four-hour intraocular pressure pattern associated with early glaucomatous changes. Invest Ophthalmol Vis Sci 2003;44:1586–1590.
24. Wilensky JT, Gieser DK, Dietsche ML, Mori MT, Zeimer R. Individual variability in the diurnal intraocular pressure curve. Ophthalmology 1993;100:940–944.
25. Gregory DS, Aviado DG, Sears ML. Cervical ganglionectomy alters the circadian rhythm of intraocular pressure in New Zealand White rabbits. Curr Eye Res 1985;4:1273–1279.
26. Smith SD, Gregory DS. A circadian rhythm of aqueous flow underlies the circadian rhythm of IOP in NZW rabbits. Invest Ophthalmol Vis Sci 1989;30:775–778.
27. Kashiwagi K, Kohno K, Tsukahara S. Effect of hospitalization on intraocular pressure in patients with normal-tension glaucoma. Ophthalmologica 2003;217:284–287.
28. Henmi T, Yamabayashi S, Furuta M, et al. Seasonal variation in intraocular pressure. Nippon Ganka Gakkai Zasshi (J Jpn Ophthalmol Soc) 1994;9:782–786.
29. Qureshi IA, Xi XR, Khan IH, Wu XD, Huang YB. Monthly measurement of intraocular pressure in normal, ocular hypertensive, and glaucoma male subjects of same age group. Chang Gung Med J 1997;20:195–200.
30. Noel C, Kabo AM, Romanet JP, Montmayeur A, Buguet A. Twenty-four-hour time course of intraocular pressure in healthy and glaucomatous Africans: relation to sleep patterns. Ophthalmology 2001;108:139–144.
31. Leydhecker W, Akiyama K, Neumann H.G. Der intraokulare Druck gesunder menschlicher Augen. Klin Monatsbl Augenheilkd 1958;133:662–670.

BRAIN RESEARCH 1109 (2006) 192–200

available at www.sciencedirect.com

ScienceDirect

www.elsevier.com/locate/brainres

BRAIN RESEARCH

Research Report

A new model of retinal photoreceptor cell degeneration induced by a chemical hypoxia-mimicking agent, cobalt chloride

Akira Hara[a,*], *Masayuki Niwa*[b,c], *Hitomi Aoki*[e], *Masako Kumada*[d], *Takahiro Kunisada*[e], *Takeru Oyama*[a], *Tetsuya Yamamoto*[d], *Osamu Kozawa*[b], *Hideki Mori*[a]

[a]*Department of Tumor Pathology, Gifu University Graduate School of Medicine, 1-1 Yanagido, Gifu 501-1194, Japan*
[b]*Department of Pharmacology, Gifu University School of Medicine, 1-1 Yanagido, Gifu 501-1194, Japan*
[c]*Medical Education Development Center, Gifu University School of Medicine, 1-1 Yanagido, Gifu 501-1194, Japan*
[d]*Department of Ophthalmology, Gifu University School of Medicine, 1-1 Yanagido, Gifu 501-1194, Japan*
[e]*Department of Tissue and Organ Development, Gifu University Graduate School of Medicine, 1-1 Yanagido, Gifu 501-1194, Japan*

ARTICLE INFO

Article history:
Accepted 14 June 2006
Available online 25 July 2006

Keywords:
Retina
Photoreceptor cell
Degeneration
Cobalt chloride
Hypoxia

ABSTRACT

Retinal photoreceptor cell degeneration was induced by cobalt chloride, a chemical hypoxia-mimicking agent in rodents. Time course and dose–response of photoreceptor cell degeneration in mouse retina after intravitreal injection of cobalt chloride were examined by conventional histological analysis by hematoxylin and eosin staining and in situ terminal dUTP-biotin nick end labeling of DNA fragments (TUNEL) method with the use of paraffin-embedded sections. The dose–response of photoreceptor cell degeneration in rat retina was also examined. Photoreceptor cells progressively degenerated with time and under dose–response relationship. The suitable dose of cobalt chloride for the selective photoreceptor cell degeneration in mice is 10–12 nmol intravitreal injection at the volume of 2 μl. The retinal morphology of the mice 2 weeks after the 10–12 nmol intravitreal injection was similar to that of retinal degeneration in the mutant *rd* mouse. Retinal damage of total retinal layers was induced by an excessive dose of cobalt chloride. The progression of retinal damage after cobalt chloride injection, measured morphologically, was completed at 1 week. However, nuclear DNA fragmentation, mainly detected at outer nuclear layer by TUNEL, peaked at 48 h after 12 nmol cobalt chloride injection. Thus, the selective photoreceptor cell degeneration induced by cobalt chloride follows DNA fragmentation at outer nuclear layer. The photoreceptor cell degeneration is established optionally by cobalt chloride without use of the retinal degeneration mutant animals. Thus, we have described the development of a new model of retinal photoreceptor cell degeneration induced by a chemical hypoxia-mimicking agent.

* *Corresponding author.* Fax: +81 58 230 6226.
E-mail address: ahara@cc.gifu-u.ac.jp (A. Hara).

0006-8993/$ – see front matter © 2006 Elsevier B.V. All rights reserved.
doi:10.1016/j.brainres.2006.06.037

1. Introduction

Retinal degenerative diseases, either acquired or inherited, are a major cause of visual impairment and blindness in humans. Most retinal degeneration caused by genetic mutations affect the retinal pigment epithelium and sensory retina. For example, retinitis pigmentosa (RP), which is characterized by a progressive loss of photoreceptors through mechanisms not yet fully understood, is a leading cause of blindness and visual disability in younger people (Berson, 1993). Mutations in a number of different genes (such as rhodopsin, the beta subunit of cGMP phosphodiesterase and peripherin) have been identified as the primary genetic lesion in different forms of human retinitis pigmentosa (Kennan et al., 2005). Age-related macular degeneration (AMD), which is a diffuse condition involving the retinal pigment epithelium, is also recognized as a complex genetic disorder in which one or more genes contribute to an individual's susceptibility for developing the condition (Green, 1999; Zack et al., 1999). The condition of these diseases is currently incurable, and there are still many obstacles that need to be overcome before treatments including gene therapy or cell replacement therapy can be applied to humans (Delyfer et al., 2004; Yu and Cringle, 2005).

Many animal models of retinal degeneration are available and have led to a better understanding of the disease and to the development of possible therapeutic strategies. A well-established animal model of retinal degeneration, rd mouse, possesses a mutation of the rod-specific phosphodiesterase and leads to the rapid and massive death of rod photoreceptors in the first few weeks of postnatal life (Bowes et al., 1990) and then leads to blindness with subsequent cone degeneration in less than 2 months (Jimenez et al., 1996). Animal models with spontaneous retinal degeneration have been used for many years to study disease progression and pathology. Many of these animal models have come from screening mice from genetically independent mouse strains (Chang et al., 1993; Hawes et al., 2000).

The involvement of the genetic aspects of retinal degeneration is well established (Berson, 1993; Chang et al., 1993; Hawes et al., 2000), but there is much less known about the environmental and metabolic aspects of the degenerative process. The loss of photoreceptors themselves will inevitably induce metabolic changes in the remaining retina. In particular, a role for the local oxygen environment within the retina has been proposed (Yu and Cringle, 2005). In animal models of photoreceptor degeneration, manipulation of environmental oxygen levels has been reported to be able to modulate the rate of photoreceptor degeneration (Maslim et al., 1997; Valter et al., 1998).

Cobalt chloride has been widely used as a hypoxia-mimicking agent in both in vivo (Badr et al., 1999) and in vitro studies (Wang and Semenza, 1993). Many reports have shown that both cobalt and hypoxia regulate a similar group of genes on a global gene expression level (Ji et al., in press; Lee et al., 2001; Vengellur et al., 2003). Cobalt is essential for human health because of its critical role in the synthesis of vitamin B12 (Roessner et al., 2001), however, excess exposure of cobalt can lead to tissue and cellular toxicity. In the present study, a new model of photoreceptor cell degeneration induced by intravitreal injection of cobalt chloride is presented.

2. Results

2.1. *Histologic evaluation of the retinal degeneration*

Photoreceptor cells progressively degenerated with time (Fig. 2) and under dose–response relationship (Figs. 1 and 3). Various retinal lesions were caused by intravitreal injection of cobalt chloride (Figs. 1, 2 and 3). To determine a suitable dose of cobalt chloride for the selective photoreceptor cell degeneration, the morphological changes characterized by hematoxylin and eosin (HE) staining in each retina were scored semi-quantitatively by microscopic examination as follows: negative, 0; minimal morphological changes of the

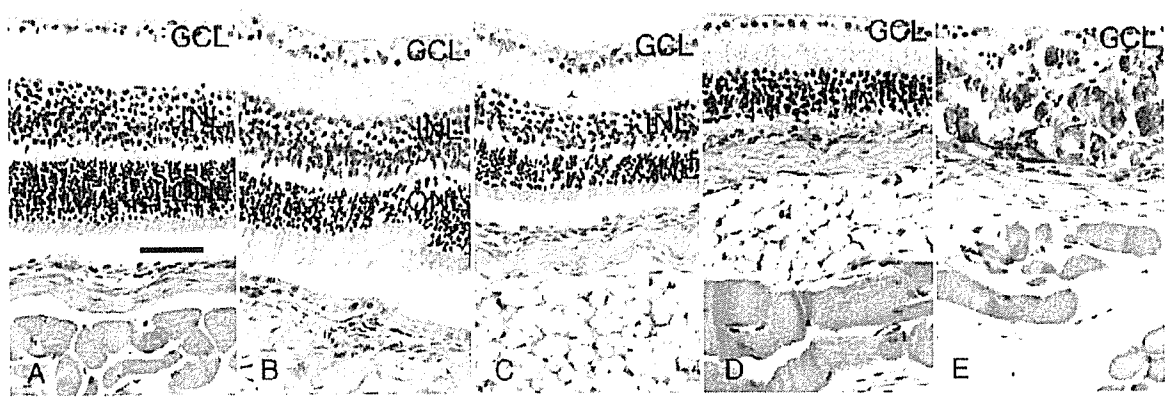

Fig. 1 – Representative microphotographs of histological examination by hematoxylin and eosin staining in mouse retina 2 weeks after treatment of each dose of cobalt chloride. (A) 1, (B) 2, (C) 5, (D) 10 and (E) 20 nmol cobalt chloride in 2 μl of distilled water was injected intravitreally. As described in Results, the cobalt-chloride-induced morphological changes in each retina were scored semi-quantitatively. In panel A, no morphological change was recognized, thus scored as 0. The morphological changes of retinal cell degeneration in panels B, C, D and E were scored 1, 2, 3 and 4, respectively. GCL, ganglion cell layer; INL, inner nuclear layer; ONL, outer nuclear layer. Scale bar in panel A, 50 μm.